Transportation Research Part D 161 (2026) 105619

Contents lists available at ScienceDirect

Transportation Research Part D

journal homepage: www.elsevier.com/locate/trd

Explaining COVID-19 Tokyo metro station-level ridership disruption and recovery: pre-pandemic demand, built environment and centrality ☆

Xi Lin [a,*], Giuseppe Vizzari [b], Claudio Feliciani [c,d], Daichi Yanagisawa [a,c,e], Katsuhiro Nishinari [a,c,e,f]

[a] Department of Advanced Interdisciplinary Studies, School of Engineering, The University of Tokyo, 4-6-1, Komaba, Meguro-ku, Tokyo 153-8904, Japan
[b] Department of Informatics, Systems and Communication, University of Milano-Bicocca, Viale Sarca 336/14, 20126 Milano, Italy
[c] Department of Aeronautics and Astronautics, School of Engineering, The University of Tokyo, 7-3-1, Hongo, Bunkyo-ku, Tokyo 113-8656, Japan
[d] Waseda Institute for Advanced Study, Waseda University, 1-21-1 Nishiwaseda, Shinjuku-ku, Tokyo 169-0051, Japan
[e] Mobility Innovation Collaborative Research Organization, The University of Tokyo, 5-1-5, Kashiwanoha, Kashiwa-shi, Chiba 277-8574, Japan
[f] Research Center for Advanced Science and Technology, The University of Tokyo, 4-6-1, Komaba, Meguro-ku, Tokyo 153-8904, Japan

A R T I C L E I N F O

Keywords:
COVID-19
Metro ridership
Built environment
Network centrality
Geographically weighted regression(GWR)

A B S T R A C T

COVID-19 caused severe and uneven metro ridership declines. This study examines station-level annual ridership change in Tokyo from 2020 to 2023 relative to 2019, integrating pre-pandemic demand, built environment, and network centrality. Its main contribution is to identify how these factors shaped ridership resilience from acute disruption to recovery using ordinary least squares (OLS) and geographically weighted regression (GWR). Results show that high pre-pandemic demand and Production and Service intensity are associated with larger proportional losses, especially in 2020–2021. Road density is consistently linked to smaller declines and stronger recovery, indicating the importance of local access networks. Land-use mix becomes increasingly positive during recovery, suggesting that functionally diverse station areas better supported localized daily activities. Destination accessibility and centrality show more spatially uneven and temporally unstable effects. These findings suggest that resilience-oriented planning should combine targeted operations for vulnerable high-demand stations with local access improvements and mixed-use station-area development.

1. Introduction

Urban rail transit is a backbone of daily mobility in many large metropolitan areas, shaping both commuting patterns and the spatial organization of activities (Li et al., 2025). The COVID-19 pandemic, recognized in disaster risk reduction frameworks as a large-scale biological-hazard disaster (Mizutori, 2025), produced an unprecedented shock to public transport demand (Kashem et al., 2021), disrupting long-established ridership patterns and raising new questions about the resilience of metro systems (Cui et al., 2025). While many cities have observed partial recoveries after the initial collapse, the pace and extent of rebound have not been uniform, and in

☆ This article is part of a special issue entitled: 'Travel in Disasters' published in Transportation Research Part D.

* Corresponding author.
E-mail address: lin-xi@g.ecc.u-tokyo.ac.jp (X. Lin).

https://doi.org/10.1016/j.trd.2026.105619
Received 27 January 2026; Received in revised form 28 July 2026; Accepted 3 September 2026
Available online 13 September 2026

some cases demand has remained below pre-pandemic levels even several years after the outbreak (Vickerman, 2021; Wilbur et al., 2023).

Importantly, the pandemic's impact has not been spatially homogeneous within a metro network (J. Li et al., 2024). Stations differ substantially in their functional roles and surrounding urban contexts, including central business districts and major transfer hubs, as well as residential neighborhoods and peripheral activity nodes. Such heterogeneity implies that system-wide averages can obscure meaningful local dynamics, and that understanding station-level variation is essential for designing targeted operational strategies and longer-term transit-oriented planning responses.

Despite the growing body of research documenting ridership change in urban rail transit systems, important limitations remain. The COVID-19 pandemic has highlighted the vulnerability of urban mobility systems to external shocks and has triggered substantial and potentially persistent changes in travel behavior (Cui et al., 2025). While a large literature has examined how the surrounding built environment shapes metro ridership under "normal" conditions (Ding et al., 2019; Yang et al., 2023b), comparatively fewer studies investigate which factors are associated with ridership change when transit systems experience abrupt disruptions caused by rare but severe disaster such as COVID-19. Moreover, much of the existing evidence is based on a single time period or a short window (Andersson et al., 2021), offering limited insight into how the determinants of ridership change evolve from the acute disruption stage to the recovery stage across multiple years. Finally, existing station-level studies often rely on a narrow set of explanatory factors, potentially overlooking how multiple dimensions jointly shape ridership and its post-pandemic change. Some emphasize rail ridership data and network patterns (Li et al., 2022) while paying limited attention to station-area context, whereas others focus mainly on built-environment and land-use attributes (Gan et al., 2020; Li et al., 2020; Karawapong et al., 2025; Li et al., 2024a; Li et al., 2025; Shao et al., 2020) or, alternatively, on network centrality alone (An et al., 2019).

To address these gaps, this study investigates the spatial heterogeneity of station-level metro ridership change in Tokyo during 2020–2023, using 2019 as baseline. We focus on the 2019–2023 period because it captures the full trajectory from the pre-pandemic baseline through the most disruptive pandemic phase and into the subsequent recovery period. Tokyo provides a compelling case because of its highly transit-oriented urban structure and the dense, multi-line metro network that underpins metropolitan mobility. The dependent variable is defined as the annual ridership change rate at each station relative to 2019, enabling a consistent comparison of the shock and recovery phases. To avoid mathematical coupling between the 2019-based dependent variable and the explanatory variables, pre-pandemic demand is measured using the 2017–2018 average annual ridership rather than 2019 ridership. Explanatory variables are constructed to represent three complementary dimensions: historical pre-pandemic demand (2017–2018 average annual ridership), built-environment characteristics, and network centrality. These factors may interact and become particularly salient in explaining heterogeneous station-level responses during COVID-19 and in the post-COVID period (Karawapong et al., 2025; Pang et al., 2023). Accordingly, this study extends the analysis of transit resilience beyond resistance to the initial shock by examining how station-area characteristics supported or constrained adaptive recovery throughout the 2020–2023 period.

Methodologically, we combine a global benchmark model with a local spatial modeling approach. We first estimate Ordinary Least Squares (OLS) models to identify candidate specifications and to assess whether spatial dependence or non-stationarity is evident. We then apply Geographically Weighted Regression (GWR) to quantify spatially varying associations between ridership change and its determinants, and to map where particular factors matter more within the metropolitan area. By estimating models separately for each year from 2020 to 2023, the analysis also reveals how spatial patterns of influence evolve from the acute disruption phase to the recovery stage.

The remainder of the paper is organized as follows. Section 2 reviews relevant literature. Section 3 describes the study area and datasets, as well as variable construction. Section 4 introduces the methodological framework. Section 5 presents results and spatial patterns of key determinants across years. Section 6 summarizes the key findings and highlights planning implications and future research needs.

2. Literature review

2.1. COVID-19-related impacts on public transport

Since the outbreak of COVID-19, transport systems worldwide have been disrupted across multiple modes, including aviation, maritime shipping, railways, and urban transport (Zhang et al., 2021). Among these, urban public transport experienced particularly severe shocks because infection risk concerns and policy interventions directly constrained shared mobility. During the early lockdown period, a combination of stay-at-home orders and social distancing measures led to an almost complete breakdown of urban transit use in many cities, with passenger demand commonly declining by approximately 80–95% (Vickerman, 2021). Although ridership rebounded gradually as restrictions were relaxed, recovery has often been slow and incomplete, with demand typically returning to only around half of pre-pandemic levels (Vickerman, 2021).

Evidence from datasets across different regions further highlights the magnitude of this collapse. In the United States, both public transit and rail ridership in 2020 fell to their lowest levels in roughly a century (Ziedan et al., 2023). At the same time, travelers' preferences shifted noticeably toward private modes, reflecting both perceived safety advantages and changing activity patterns (Kamga and Eickemeyer, 2021). However, declines were not uniform across population groups or trip purposes. Many commuters, especially those unable to work from home, continued to rely on metro systems as an essential travel option (Basu and Ferreira, 2021). Consistent with risk-sensitive behavior, metro demand has also been shown to respond to epidemic severity in real time. For example, in Taipei, each additional newly confirmed COVID-19 case was associated with a 1.43% reduction in metro trips (Chang et al., 2021).

Beyond short-term disruption, a growing body of research suggests that the pandemic may generate persistent or even structural changes in lifestyles and travel behavior, including long-lasting shifts in commuting and daily routines (Balbontin et al., 2021; Thomas et al., 2021). Moreover, mobility responses have been linked to broader social and political contexts. For instance, variations in travel reduction have been associated with political orientation and poverty levels (Kim and Kwan, 2021). Finally, pandemic-driven changes in activity patterns have implications not only for transport demand but also for urban systems more broadly, potentially reshaping the built environment and the spatial distribution of places and activities over time (de Palma et al., 2022).

2.2. Determinants of metro ridership under normal conditions

Metro ridership is associated with socio-demographics, environmental conditions, neighborhood composition, and the built environment. Age structure is linked to ridership (Li et al., 2024a), and weather can affect transit passenger volumes (Kalkstein et al., 2009; Singhal et al., 2014). Ridership also varies with neighborhood racial composition (Chen et al., 2009) and with housing prices and gentrification processes (Chava et al., 2018; Yan et al., 2023). Pedestrian infrastructure such as marked crosswalks is another relevant correlate (Li and Rodriguez, 2024). Built-environment characteristics are repeatedly identified as key determinants (Karawapong et al., 2025; Li et al., 2020, 2025; Pang et al., 2023), and network structure and station centrality further shape station demand (An et al., 2019; Pang et al., 2023). Metro ridership is also influenced by multimodal integration, including cycling and bike sharing as complementary access modes (Gao et al., 2022; Zhao et al., 2013), and by Transit-Oriented Development (TOD) functionality, especially through interactions between node characteristics and functional performance (Su et al., 2022).

More specifically, housing-market evidence indicates that gentrification and higher housing prices can contribute significantly to metro ridership growth (Chava et al., 2018; Yan et al., 2023). Station-area activity intensity also matters, since commercial, industrial, residential, transport-related, and attraction-related factors are often positively associated with ridership (Karawapong et al., 2025). Local transport supply can reshape these effects, and higher densities of branch roads and bus stops may reduce reliance on metro for short-distance trips (Li et al., 2025). Station accessibility remains important, and both higher-quality access and a larger number of station entrances are positively associated with rail ridership (Li et al., 2020). Evidence from Shenzhen further suggests that greater road density encourages higher ridership in both metro and bus systems (Tu et al., 2018).

Network structure also conditions station demand, and betweenness centrality is positively associated with Shanghai metro ridership (An et al., 2019). The relevance of accessibility and network effects varies by station function, since destination accessibility and centrality are primarily significant for employment-oriented and employment-mixed stations (Pang et al., 2023). Trip purpose further differentiates predictors, because bus stop counts strongly predict commuting ridership, whereas residential and community services, road density, and leisure and entertainment facilities play a larger role in non-commuting ridership (Li et al., 2024b). Cross-city evidence also cautions against assuming universal spatial gradients, because distance to the city center is not a significant determinant of station ridership in Nanjing (Zhao et al., 2014).

Multimodal connectivity has become increasingly central in ridership research. Bike sharing complements metro by improving last-mile access, and its ridership-enhancing effects are stronger in peripheral areas than in central areas (Gao et al., 2022). Intermodal integration also matters, since additional bicycle park-and-ride capacity and convenient metro-bus transfers can promote metro use (Zhao et al., 2013). In Shanghai, ridership is explained more by TOD functionality, particularly through its interaction with node characteristics, than by land-use factors alone (Su et al., 2022).

2.3. Determinants of metro ridership change during COVID-19

COVID-19 produced an abrupt and large-scale disruption to public transport demand, and metro ridership change during the pandemic is not simply a scaled-down version of normal ridership variation. Early interventions such as lockdowns and social-distancing measures sharply reduced passenger demand (Vickerman, 2021). However, the decline exhibited strong spatial and social heterogeneity. Areas with higher proportions of essential workers and vulnerable populations tended to maintain higher levels of minimal metro demand during COVID-19 (Liu et al., 2020). Higher levels of coronavirus-related Google searches were also associated with higher residual demand (Liu et al., 2020). Evidence further suggests that commuting behavior among some minority groups was less affected by the pandemic (Xiao et al., 2022).

Pandemic severity indicators can also influence demand in near real time. Newly confirmed COVID-19 cases have been reported to significantly affect metro ridership (Chang et al., 2021). Station-area correlates of ridership can shift during the pandemic period as well. In Wuhan, residential population, the number of nearby bus stops, the number of enterprises around stations, and whether a station is a transfer station all show positive associations with metro ridership. In contrast, street length, the number of restaurants, and the number of station exits show negative associations (Yang et al., 2023a). In addition to cross-sectional modeling, time-series approaches have been adopted to characterize dynamic patterns during COVID-19. An ARIMA-based linear non-stationary time-series model has been used to capture temporal variation in metro ridership during the pandemic (Moghimi et al., 2023).

3. Study area and data

3.1. Study area

Tokyo, Japan's capital, is a highly transit-oriented megacity where rail transit underpins daily mobility. Within the Tokyo administrative boundary, metro services are primarily provided by two operators: Tokyo Metro Co., Ltd and the Toei Subway (Bureau of Transportation, Tokyo Metropolitan Government). Tokyo Metro operates 9 lines, while the Toei Subway operates 4 lines. Fig. 1(a) presents the complete metro network operated by these two operators. Because several metro stations on these lines are located outside the administrative boundary of Tokyo Metropolis, we exclude them to ensure consistency with Tokyo-based statistical datasets used in this study. Specifically, eight stations outside Tokyo are removed from the study sample: F01/Y01 Wakoshi, S21 Motoyawata, T18 Urayasu, T19 Minami-gyotoku, T20 Gyotoku, T21 Myoden, T22 Baraki-nakayama, and T23 Nishi-funabashi.

The regression analysis covers the five-year period from 2019 to 2023. During this period, Toranomon hills station (H06) opened on June 6, 2020, and was formally incorporated into Tokyo's annual statistical reporting starting in 2021. Accordingly, the within-Tokyo metro network is defined in a year-sensitive manner: the network used for later years (2021–2023) includes H06 (Fig. 1(b), with its location highlighted), whereas the network used for earlier years (2019–2020) follows the within-Tokyo station set that does not include H06 in the official statistics (Fig. 1(c)).

Accordingly, in the regression analysis, Toranomon Hills (H06) is excluded from any variables that require a 2019 baseline. Specifically, because H06 is not included in the official station statistics for 2019–2020, it is omitted when constructing year-over-year measures relative to 2019 (e.g., the annual ridership change rate). In addition, because the station set differs between the two periods, network-derived variables are computed using year-specific metro graphs. As a result, centrality measures for 2021–2023 are calculated on the updated network that includes H06, and they are not directly identical to those computed for 2019–2020 on the earlier network.

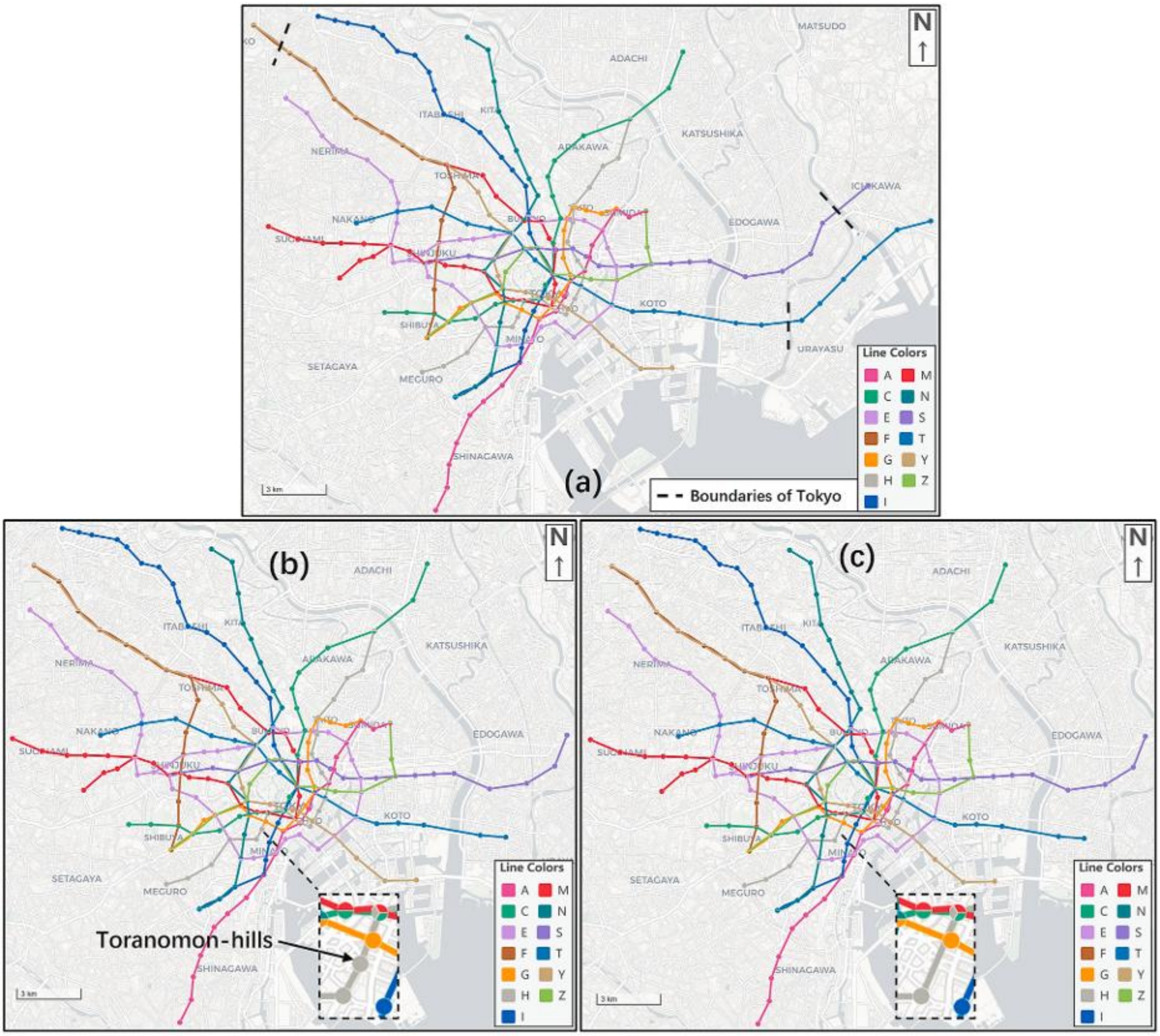

Fig. 1. Tokyo metro network: (a) Full network. (b) Within-Tokyo network for 2021–2023 (includes H06). (c) Within-Tokyo network for 2019–2020 (excludes H06).

3.2. Data

3.2.1. Data sources

All datasets used in this study were collected from publicly available online open-source platforms and official statistical portals. As summarized in Table 1, metro station names, line information, and network connectivity were compiled from the official websites of Tokyo Metro Co., Ltd. and the Bureau of Transportation, Tokyo Metropolitan Government (Toei). Station geographic coordinates, inter-station operating distances, and street-network indicators (road density and average street segment length) were derived from OpenStreetMap (OSM). Station-level annual passenger volumes were obtained from the Tokyo Statistical Yearbook, ensuring consistency with official metropolitan statistics. Urban points of interest (POIs) were collected from Foursquare OS Places to characterize the built environment around stations. For cartographic visualization, basemap styling was supported by OpenStreetMap Carto.

3.2.2. Ridership

Annual station ridership for the Tokyo metro network was obtained from the Tokyo Statistical Yearbook. In this study, the dependent variable captures the station-level ridership change during the pandemic period and is defined as the annual ridership change rate $R_t(i)$ at station i in year t:

$$R_t(i) = \frac{P_t(i) - P_{2019}(i)}{P_{2019}(i)}, \tag{1}$$

where, $P_t(i)$ is the annual ridership at station i in year t (2020–2023), and $P_{2019}(i)$ is the annual ridership of station i in 2019.

Fig. 2(a) presents the yearly distribution of the annual ridership change rate $R_t(i)$ across stations, using 2019 as the baseline. A pronounced downward shift is observed in 2020, indicating a widespread ridership contraction following the onset of the pandemic. The distribution then progressively moves upward from 2021 to 2023, reflecting a gradual recovery in metro demand. Nevertheless, the bulk of stations remain below the baseline in 2023, suggesting that ridership had not fully returned to pre-pandemic levels. The persistent spread of distributions also highlights substantial station-level heterogeneity, with some stations experiencing markedly larger declines than others.

In this study, pre-pandemic demand is used as one of the independent variables and is defined as the 2017–2018 average annual ridership at each station. This specification is adopted to avoid the potential mechanical correlation that may arise when the dependent variable is defined relative to 2019 ridership while 2019 ridership is simultaneously included as an explanatory variable. Using the two-year pre-pandemic average also helps smooth short-term fluctuations in station-level demand and provides a more stable measure of baseline ridership conditions prior to the pandemic. Its spatial distribution is illustrated in Fig. 2(b). The 2017–2018 average ridership shows strong inter-station heterogeneity, with a small number of major transfer and activity hubs concentrating substantially higher demand than the rest of the network, such as Shibuya, Shinjuku, Kita-senju, and Ikebukuro.

3.2.3. Built environment

The built environment surrounding metro stations shapes travel behavior by influencing activity intensity, land-use structure, and the ease of accessing destinations. In this study, built-environment indicators are organized according to the widely used 4D framework: Density/Intensity, Diversity, Destination accessibility, and Design. To operationalize these dimensions, we first compiled points of interest (POIs), which serve as a granular proxy for local activity opportunities and functional land-use composition. POI-based measures were subsequently used to quantify intensity and diversity of surrounding urban functions, as well as to characterize destination opportunities within station catchments.

POI records were obtained from Foursquare Open-Source Places (OS Places), an open dataset that provides place locations with coordinates (WGS84), address-related fields, web/contact references, and category labels. We collected the Tokyo-area POIs in September 2025 from the OS Places parquet release hosted via a public Amazon S3 bucket. Data were extracted using a Python notebook in Google Colab, where DuckDB was used to query the parquet files directly and filter records within an expanded Tokyo bounding box (longitude 139.565001–139.959047, latitude 35.541581–35.837119). This procedure yielded approximately 1.2 million POI records for the study region. Since the extraction was performed, Foursquare has migrated OS Places delivery from the public S3 bucket to a dedicated Places portal. However, the acquisition logic remains conceptually unchanged (i.e., filtering the same underlying place records by spatial extent).

Table 1
Data sources and descriptions.

Data	Source Description	Source URL
Tokyo metro station names, line names, and connections	Tokyo Metro official website; Toei official website	https://www.tokyometro.jp/index.html; https://www.kotsu.metro.tokyo.jp/
Geographical coordinates of stations	OpenStreetMap	https://www.openstreetmap.org/
Operation distances between stations	OpenStreetMap	https://www.openstreetmap.org/
Annual passenger volume of stations	Tokyo Statistical Yearbook	https://www.toukei.metro.tokyo.lg.jp/tnenkan/tn-eindex.htm
Annual Tokyo POI data	Foursquare OS Places	https://opensource.foursquare.com/os-places/
Road density/Average street segment length	OpenStreetMap	https://www.openstreetmap.org/
Map data	OpenStreetMap Carto	https://github.com/openstreetmap-carto/openstreetmap-carto

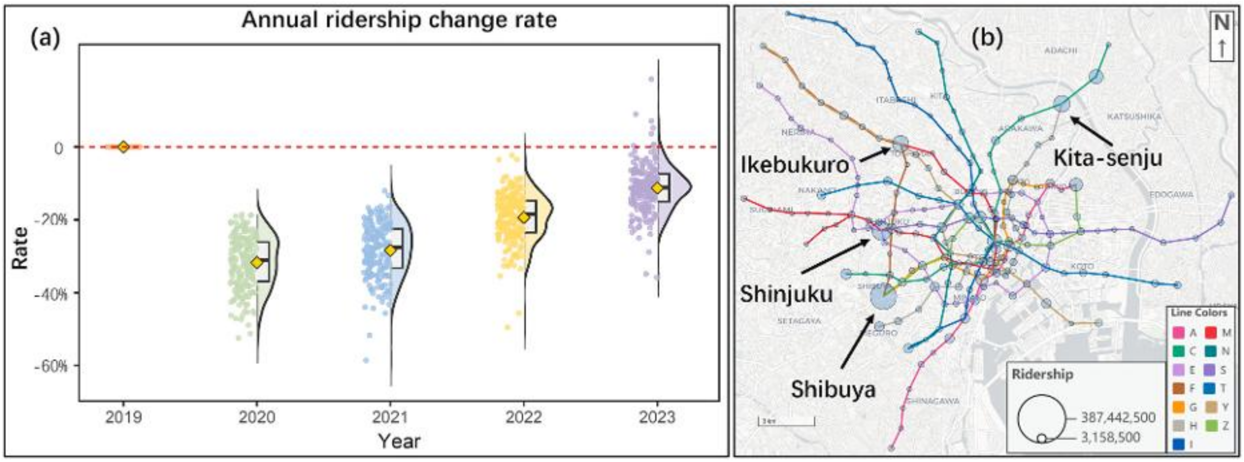

Fig. 2. (a) Yearly distribution of ridership change rate. (b) Spatial distribution of pre-pandemic ridership.

The OS Places dataset also provides temporal attributes, including creation and termination timestamps, which allows constructing time-specific snapshots (e.g., annual POI subsets aligned with the study period). In addition, POIs are associated with a predefined categorical scheme (ten major categories), while a small subset remains uncategorized.

To handle POIs with missing category labels, we applied a name-based classification procedure following the workflow illustrated in Fig. 3. Specifically, POI names were first normalized, after which a two-stage classifier was used to assign one of the predefined categories. In the first stage, high-precision rule-based matching (e.g., regular expressions capturing common Japanese/English tokens indicative of specific place types) was applied. POIs that did not match any rule were then classified in a second, model-based stage using a statistical text classifier.

The model-based component represents each POI name using character-level n-grams and Term Frequency-Inverse Document Frequency (TF-IDF) weighting. TF-IDF, widely used in text analytics, quantifies the salience of terms by up-weighting those that occur frequently within a given text while down-weighting terms that are common across the corpus (Sabbah et al., 2017). Building on these TF-IDF features, we trained a linear Support Vector Machine (SVM) to predict the most likely category for each uncategorized POI, thereby producing a complete categorical dataset for subsequent built-environment indicator construction.

After completing POI categorization, all places were assigned category labels. Note that a subset of POIs may be associated with multiple categories, reflecting multifunctional venues or overlapping activity types. The ten categories are Arts and Entertainment, Business and Professional Services, Community and Government, Health and Medicine, Dining and Drinking, Travel and

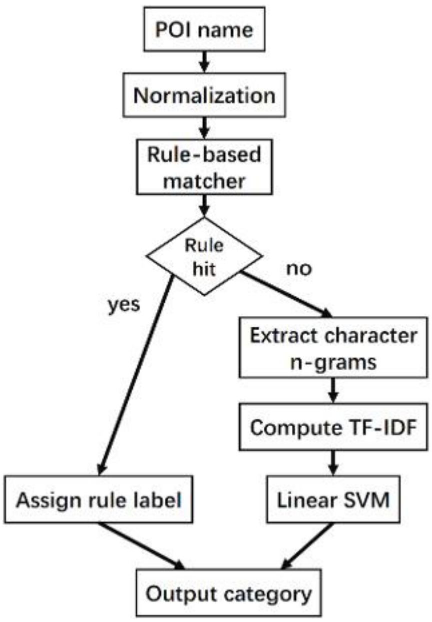

Fig. 3. Workflow for imputing missing POI categories.

Transportation, Retail, Sports and Recreation, Landmarks and Outdoors, and Event. The spatial distribution of POIs across Tokyo in 2023 is illustrated in Fig. 4(a).

To measure station-area activity opportunities, we delineated a 1 km buffer around each metro station centroid (Fig. 4(b)), which approximates a 15-minute walking catchment (Shi et al., 2025). For each station, we counted the number of POIs within the buffer by category and used these counts to construct POI-based built-environment indicators.

Applying the same buffer-based aggregation procedure to each year of the study period (2020–2023), we generated annual station-level summaries of total POI counts (and category-specific counts) within the 1 km catchment. These yearly POI statistics form the basis for constructing time-aligned built-environment indicators and are reported in Table 2. Because the Event category primarily represents temporary or episodic activities (e.g., venues associated with event hosting) rather than stable urban functions, it was excluded from subsequent built-environment measurements and model specifications.

Within the built environment 4D framework, Density/Intensity is operationalized using four POI-based measures derived from the 1 km station catchments. First, we compute the total number of POIs within each station buffer, aggregating across the nine retained categories. Second, we construct a Production and Service variable, defined as the sum of POIs in Business and Professional Services, Community and Government, and Health and Medicine, capturing employment-oriented and public-service functions. Third, we define a Consumption and Leisure variable as the combined count of POIs in Dining and Drinking, Retail, Arts and Entertainment, and Sports and Recreation, reflecting consumption activities and leisure opportunities. Finally, we derive a Mobility and Outdoor variable by summing POIs in Travel and Transportation and Landmarks and Outdoors, capturing the concentration of mobility-supporting facilities together with outdoor and amenity-oriented destinations around each station.

Within the built environment 4D framework, Diversity is captured using the degree of land use mix (LUM) within each station catchment. Following an entropy-based formulation, LUM is computed as:

$$L_i = -\sum_{i=1}^{9} p_i \times \log_9(p_i), \tag{2}$$

where, p_i is the share of POIs in category i among all POIs within the 1 km buffer.

Within the built environment 4D framework, destination accessibility is proxied by each station's distance to the nearest major metropolitan center, reflecting Tokyo's polycentric urban structure rather than assuming a single central destination. Specifically, five major centers in the metropolitan rail system are considered: Tokyo Station, Ueno, Shinjuku, Shibuya, and Ikebukuro stations. For each station i, the central accessibility indicator, denoted as d_i^{CBD}, is defined as the minimum great-circle (geodesic) distance from the station centroid to any of these centers, calculated using the Haversine formula:

$$d_{ic} = 2r\arcsin\left(\sqrt{\sin^2\left(\frac{\phi_i - \phi_c}{2}\right) + \cos(\phi_i)\cos(\phi_c)\sin^2\left(\frac{\lambda_i - \lambda_c}{2}\right)}\right), \tag{3}$$

$$d_i^{\text{CBD}} = \min_{c \in \mathscr{C}} d_{ic}, \quad C = \{\text{Tokyo}, \text{Ueno}, \text{Shinjuku}, \text{Shibuya}, \text{Ikebukuro}\}. \tag{4}$$

where, d_{ic} is the geodesic distance from station i to center $\mathscr{C}$, r is the Earth's radius, ϕ denotes latitude, and λ denotes longitude (in radians). Smaller values of d_i^{CBD} indicate higher central accessibility, whereas larger values reflect a more peripheral station location

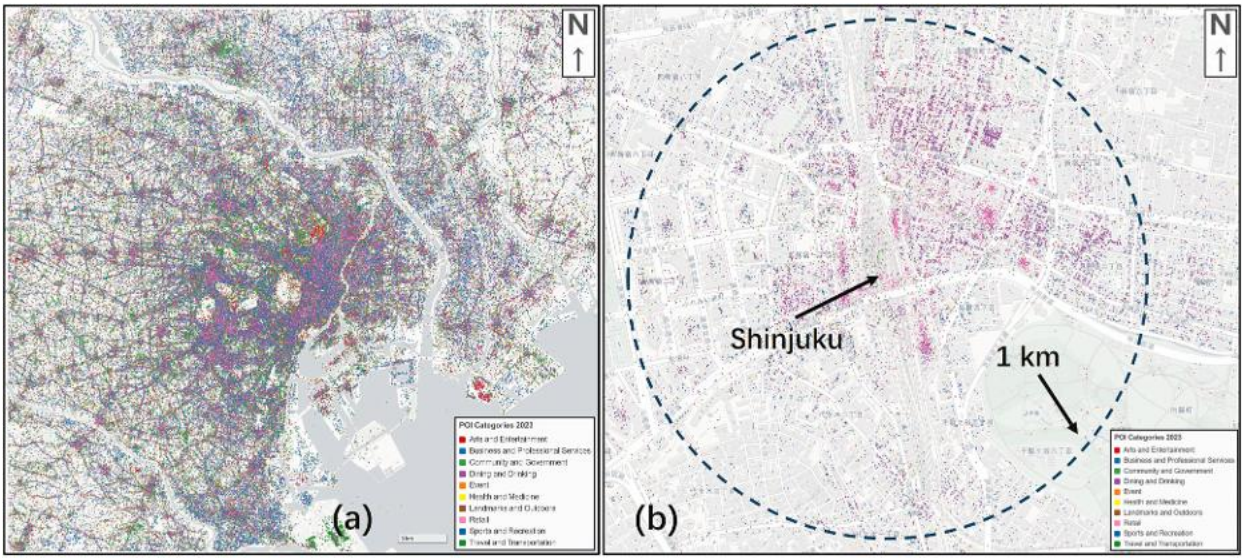

Fig. 4. (a) Spatial distribution of POIs across Tokyo (2023 shown). (b) 1 km buffer around a metro station centroid (Shinjuku shown).

Table 2
Yearly POI statistics.

POI	2020		2021		2022		2023	
	Mean	SD	Mean	SD	Mean	SD	Mean	SD
Arts and Entertainment	244.8	266.38	254.1	273.46	262.02	282.99	269.58	288.89
Business and Professional Services	1784.45	1443.36	1949.54	1579.54	2017.95	1639.24	2049.66	1668.62
Community and Government	412.57	254.62	437.8	269.96	450.75	277.89	464.21	289.62
Dining and Drinking	2527.47	2470.68	2710.49	2630.42	2807.48	2734.36	2869.32	2789.3
Health and Medicine	230.29	142.74	250.34	156.84	259.67	164.12	268.71	170.19
Landmarks and Outdoors	334.55	263.9	351.67	274.19	363.12	280.98	375.41	288.54
Retail	1308.22	1243.65	1385.08	1316.29	1429.18	1361.01	1451.41	1392.02
Sports and Recreation	55.75	40.04	60.55	43.45	65.03	47.22	70.44	50.66
Travel and Transportation	358.84	274.52	379.51	286.82	397.36	301.34	413.64	315.09

relative to the major urban centers.

Within the built environment 4D framework, Design is represented by two street-network variables: road density (RD) and average street segment length (SL). Both variables were derived from OpenStreetMap using R, by querying road polylines through the OSM API,

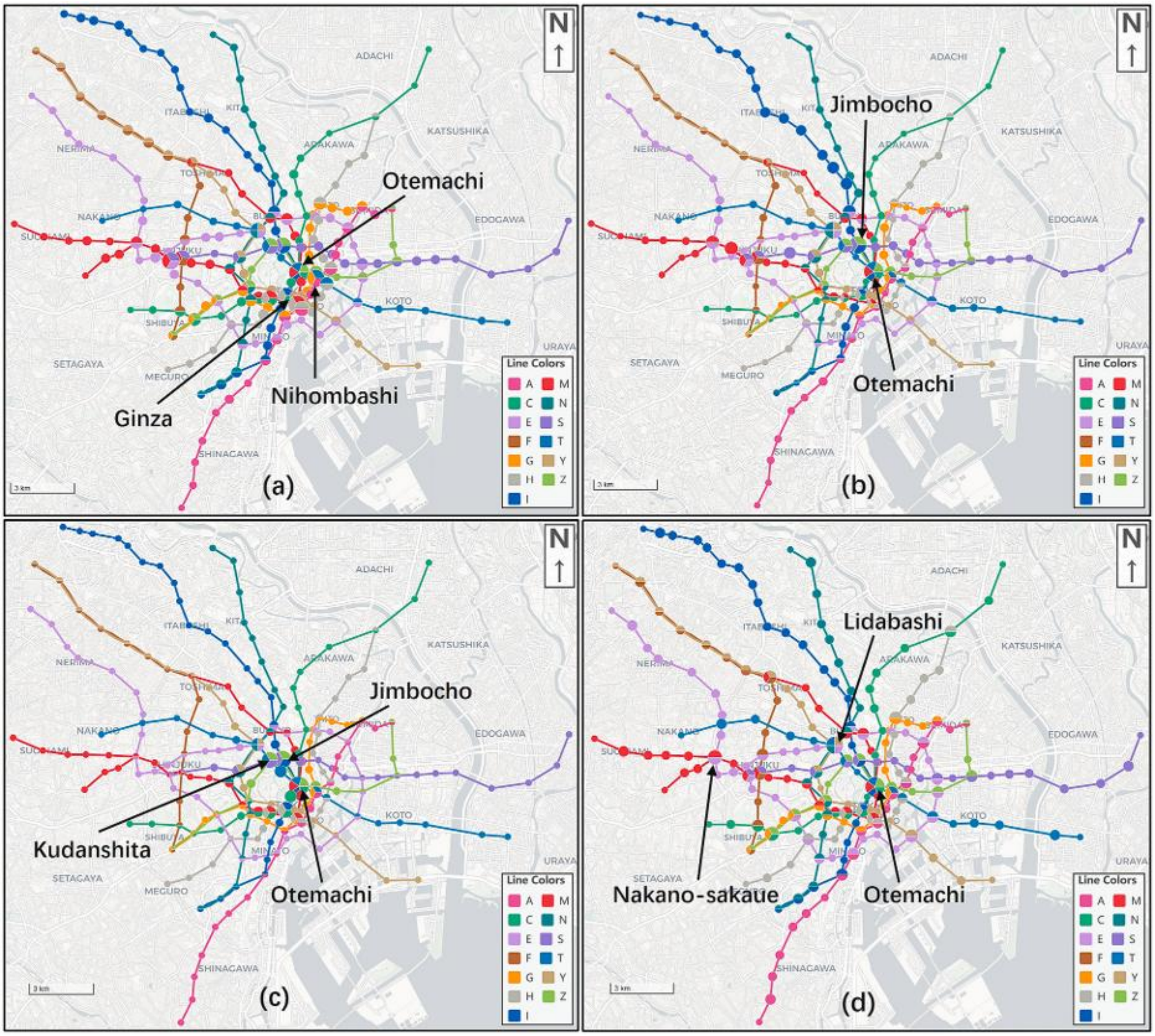

Fig. 5. Spatial distributions of station centrality measures in 2023: (a) Strength degree centrality. (b) Betweenness centrality. (c) Eigenvector centrality. (d) PageRank.

intersecting the road network with each station's 1 km buffer, and computing summary metrics within the catchment. RD was computed as the total length of road centerlines within the buffer divided by the buffer area, while SL was calculated as the mean length of road segments within the buffer (i.e., the average length of the intersected road geometries).

3.2.4. Centrality

To quantify each station's structural importance in the metro network, we constructed a station-to-station graph and computed four node-level centrality measures:

(1) Strength degree centrality. To incorporate the impedance of travel between adjacent stations, we defined an edge weight w_{ij} as the inverse of operational distance d_{ij} and computed node strength as:

$$S_i = \sum\nolimits_{j \in \mathscr{N}(i)} w_{ij} = \sum\nolimits_{j \in \mathscr{N}(i)} \frac{1}{d_{ij}}, \tag{5}$$

where, $\mathscr{N}(i)$ denotes the neighbor set of station i. Larger values indicate stations connected to many nearby neighbors (short links) and/or multiple connections.

(2) Betweenness centrality. Betweenness measures the extent to which a station lies on shortest paths between other stations:

$$B_i = \sum\nolimits_{s \neq t \neq i} \frac{\sigma_{st}(i)}{\sigma_{st}}, \tag{6}$$

where, σ_{st} is the number of shortest paths weighted with operational distance between stations s and t (computed by minimizing total path length). $\sigma_{st}(i)$ is the number of those shortest paths that pass through station i.

(3) Eigenvector centrality. Eigenvector centrality captures higher-order influence by assigning higher scores to stations connected to other highly central stations. It is defined by the leading-eigenvector solution:

Table 3
Summary of variables and descriptive statistics.

Variable	Variable description	Mean	SD
Pre-pandemic demand			
2017–2018 Average ridership (PV)	Average annual station ridership of Tokyo metro during 2017–2018 (thousand).	36145.62	45273.96
Built environment (Density/Intensity)			
2020 POI total (POI)	The number of corresponding POIs within 1 km in the corresponding year.	7256.96	6108.77
2020 Production and Service (PS)		2427.32	1759.72
2020 Consumption and Leisure (CL)		4136.24	3925.67
2020 Mobility and Outdoor (MO)		693.39	526.06
2021 POI total (POI)		7779.09	6526.37
2021 Production and Service (PS)		2637.68	1923.55
2021 Consumption and Leisure (CL)		4410.22	4163.81
2021 Mobility and Outdoor (MO)		731.19	548.27
2022 POI total (POI)		8052.56	6771.66
2022 Production and Service (PS)		2728.38	1993.89
2022 Consumption and Leisure (CL)		4563.71	4320
2022 Mobility and Outdoor (MO)		760.48	569.19
2023 POI total (POI)		8232.38	6922.97
2023 Production and Service (PS)		2782.59	2035.51
2023 Consumption and Leisure (CL)		4660.74	4412.26
2023 Mobility and Outdoor (MO)		789.05	590.26
Built environment (Diversity)			
2020 Degree of land use mix (LUM)	Degree of mixed land use within 1 km in the corresponding year.	0.8023	0.0387
2021 Degree of land use mix (LUM)		0.8008	0.0392
2022 Degree of land use mix (LUM)		0.8016	0.0399
2023 Degree of land use mix (LUM)		0.8044	0.0404
Built environment (Destination accessibility)			
Distance to center (D-CBD)	Minimum Haversine distance from each station centroid to center $\mathscr{C}$ (km).	3.0565	2.2737
Built environment (Design)			
Road density (RD)	Total road length within 1 km buffer divided by the buffer area (km/km^2).	31.14259	5.496928
Average street segment length (SL)	Mean length of road segments within 1 km buffer (m).	103.2442	23.03144
Centrality			
2020 Strength (ST)	Corresponding centrality of station in 2020 (old network).	0.207415	0.165473
2020 Betweenness (BE)		0.139097	0.150957
2020 Eigenvector (EV)		0.062076	0.141891
2020 PageRank (PR)		0.208411	0.149461
2021–2023 Strength (ST)	Corresponding centrality of station after 2020 (new network).	0.208454	0.166419
2021–2023 Betweenness (BE)		0.137931	0.149846
2021–2023 Eigenvector (EV)		0.061466	0.141476
2021–2023 PageRank (PR)		0.208009	0.14944

$$x_i = \frac{1}{\lambda}\sum_{j\in V} a_{ij}x_j, \tag{7}$$

where, λ is the largest eigenvalue of the adjacency matrix $A = [a_{ij}]$. V is set of stations.

(4) PageRank. PageRank provides a random-walk-based measure of prominence. It can be expressed as:

$$PR_i = \frac{1-\alpha}{|V|} + \alpha\sum_{j\in\mathcal{N}(i)} \frac{PR_j}{k_j}, \tag{8}$$

where, α is damping factor (typically in (0,1)), $|V|$ is the number of nodes in the network (total stations). k_j is the number of outgoing links from station j.

After computing the four centrality measures for the Tokyo metro network, Fig. 5 visualizes their spatial patterns by mapping station-level centrality magnitudes in 2023.

3.2.5. Summary of variables and descriptive statistics

This section summarizes the definitions of all variables and reports their descriptive statistics, as shown in Table 3. Among all variables, PV, POI, PS, CL, and MO are strictly positive and exhibit pronounced right-skewness (skewness > 1). Therefore, we applied natural-log transformations to these variables in subsequent regression analyses. The log transformation helps reduce skewness and the influence of extreme values, and it can also stabilize variance, thereby improving the suitability of linear modeling and the interpretability of estimated effects. In addition, before conducting both the OLS and GWR regressions, all explanatory variables were standardized using z-score transformation. This procedure places variables measured on different scales onto a common standardized scale, allowing the estimated coefficients to be more directly comparable across variables and reducing the influence of differences in measurement units. The dependent variable, namely the station-level ridership change rate relative to 2019, was not standardized and was kept in its original scale for interpretation.

4. Methods

4.1. Methodological framework

Fig. 6 illustrates the methodological framework of this study. The dependent variable is the station-level annual ridership change rate relative to the 2019 baseline, as defined in Section 3.2.2. Explanatory variables are organized into three variable groups: pre-pandemic demand, built environment, and network centrality. Pre-pandemic demand is proxied by average annual station ridership of Tokyo metro during 2017–2018. Built-environment characteristics are operationalized using the 4D framework, and one

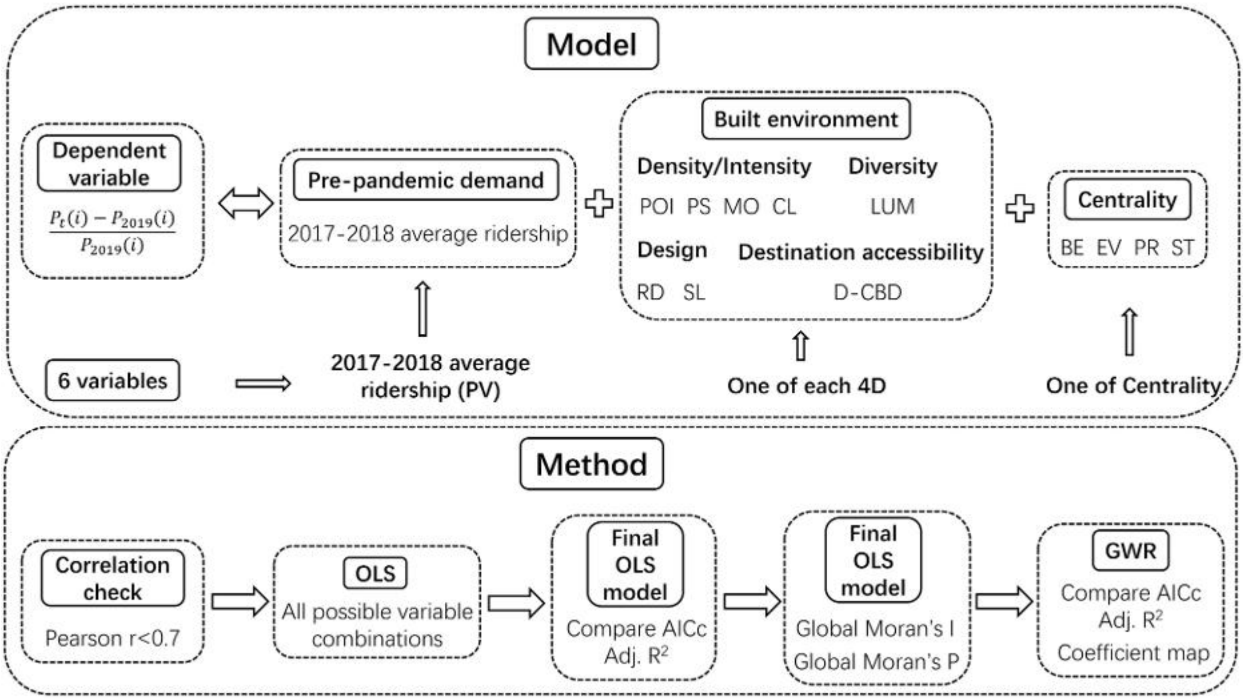

Fig. 6. Methodological framework.

variable is selected from each 4D dimension in model specification. Network structure is represented by four station-level centrality variables, from which one centrality measure is selected for inclusion in each model. As a result, each final model includes six explanatory variables.

Model estimation follows a multi-step workflow. First, we conducted a pairwise correlation screening and removed predictors exhibiting high collinearity. Second, we estimated OLS models consistent with the structure in Fig. 6 and compared candidate specifications using AICc and adjusted R^2 to select the final global model. Third, we assessed residual spatial dependence in the selected OLS model using global Moran's I and its associated significance test. Finally, we applied GWR to allow coefficients to vary across space, evaluated GWR against OLS using AICc and adjusted R^2, and examined spatial heterogeneity through maps of local coefficients.

4.2. Ordinary least squares (OLS) regression

Ordinary least squares (OLS) is a global regression approach that estimates a single set of coefficients for the entire study area, capturing overall trends and average relationships while ignoring spatial heterogeneity. The OLS model is specified as:

$$y_i = \beta_0 + \sum_{k=1}^{p} \beta_k x_{ik} + \varepsilon_i. \tag{9}$$

where, y_i denotes the dependent variable for station i (the annual ridership change rate relative to 2019), x_{ik} is the k-th explanatory variable for station i, β_0 and β_k are global parameters, p is the number of explanatory variables, and ε_i is the error term.

Following the structure in Fig. 6, each final specification includes six explanatory variables (pre-pandemic ridership, one variable from each 4D dimension, and one centrality measure). Candidate OLS models were compared using AICc and adjusted R^2 to identify the final global model.

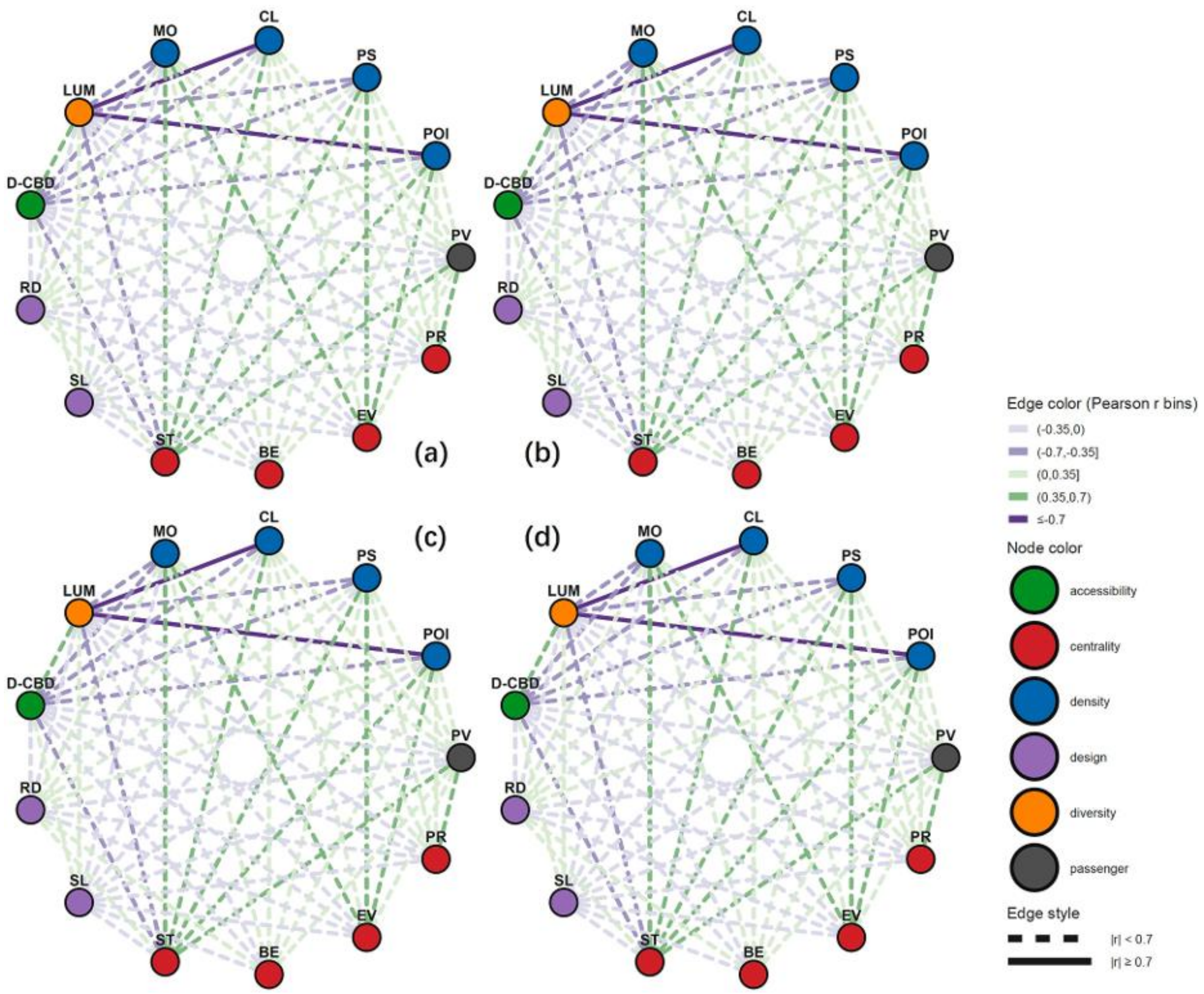

Fig. 7. Pairwise Pearson correlation of all candidate explanatory variables in (a) 2020, (b) 2021, (c) 2022, (d) 2023.

4.3. Geographically weighted regression (GWR)

Geographically weighted regression (GWR) extends OLS by allowing relationships to vary across space, thereby capturing local heterogeneity. The GWR model is expressed as:

$$y_i = \beta_0(u_i, v_i) + \sum_{k=1}^{p} \beta_k(u_i, v_i) x_{ik} + \varepsilon_i. \tag{10}$$

where, (u_i, v_i) are the spatial coordinates of station i, and $\beta_k(u_i, v_i)$ are location-specific coefficients estimated using spatial weighting around each station. Model performance was evaluated by comparing GWR with the selected OLS benchmark using AICc and adjusted R^2, and spatial heterogeneity was interpreted through maps of local coefficients. In this study, GWR was estimated using an adaptive bisquare kernel, and the optimal bandwidth was selected by minimizing AICc.

5. Results

5.1. Correlation check

To reduce multicollinearity and ensure stable coefficient estimation, we conducted a pairwise Pearson correlation screening among all candidate explanatory variables. Correlations were calculated for all feasible variable pairs under the modeling structure, and the results are summarized in Fig. 7.

Across all year-specific model settings, the correlation patterns were highly consistent. In particular, land use mix (LUM) exhibited a strong correlation with Consumption and Leisure (CL) and with total POI (POI) in each year. Therefore, to avoid including highly collinear predictors in the same specification, we exclude model combinations that simultaneously include LUM with CL or LUM with POI.

5.2. Model selection

Based on the correlation screening in Section 5.1, we enumerated all feasible OLS specifications under the framework in Fig. 6. Given the rule that each model includes pre-pandemic ridership, one variable from each 4D dimension, and one centrality measure, and that collinear pairings are excluded, there are 16 admissible model combinations.

Table 4 reports the top five model specifications for each year (2020–2023, relative to the 2019 baseline). The model label reports only the three varying components: Density/Intensity, Design, and Centrality. PV, LUM, and D-CBD are included in all candidate models.

Although the year-specific best models vary, the specification including Production and Service (PS), road density (RD), and betweenness centrality (BE) appears among the top five in all years. Therefore, PS-RD-BE is selected as the final global OLS model to maintain cross-year comparability and to focus on interpretable, temporally consistent determinants. This specification includes pre-pandemic ridership (PV), Production and Service (PS) (Density/Intensity), Road density (RD) (Design), Degree of land use mix (LUM) (Diversity), Distance to center (D-CBD) (Destination accessibility), and Betweenness centrality (BE) (Network centrality).

Table 4
Top five OLS model specifications across four years.

	Rank	Model	R^2	Adj. R^2	AICc
2020	**1**	**PS-RD-BE**	**0.495**	**0.480**	**−628.190**
	2	PS-RD-EV	0.494	0.478	−627.693
	3	PS-RD-ST	0.493	0.478	−627.595
	4	PS-RD-PR	0.493	0.477	−627.277
	5	MO-RD-ST	0.472	0.456	−619.190
2021	1	MO-RD-BE	0.551	0.538	−642.513
	2	MO-RD-ST	0.548	0.535	−641.219
	3	MO-RD-PR	0.548	0.535	−641.168
	4	MO-RD-EV	0.548	0.534	−641.060
	5	**PS-RD-BE**	**0.530**	**0.516**	**−632.984**
2022	1	MO-RD-BE	0.496	0.481	−659.845
	2	MO-RD-EV	0.489	0.474	−657.195
	3	MO-RD-PR	0.489	0.474	−657.009
	4	MO-RD-ST	0.488	0.472	−656.608
	5	**PS-RD-BE**	**0.478**	**0.463**	**−652.840**
2023	1	PS-RD-PR	0.389	0.371	−622.275
	2	**PS-RD-BE**	**0.389**	**0.371**	**−622.159**
	3	PS-RD-ST	0.386	0.368	−621.190
	4	PS-RD-EV	0.385	0.367	−620.852
	5	MO-RD-PR	0.384	0.365	−620.432

5.3. OLS results

Table 5 reports the estimated coefficients of the selected global OLS specification (PS-RD-BE) for each year from 2020 to 2023, with ridership change measured relative to the 2019 baseline.

Road density (RD) is consistently positive and statistically significant across all years, indicating that stations embedded in denser street networks tended to experience smaller ridership losses and stronger recovery relative to 2019. Pre-pandemic demand (PV) shows a consistently negative and highly significant association, suggesting that stations with higher historical pre-pandemic ridership experienced larger proportional declines. Production and Service (PS) is also negative and statistically significant in every year, implying that areas with stronger production/service intensity were more strongly associated with ridership reductions, especially during the early pandemic period. Land use mix (LUM) is not significant in 2020–2021, but becomes positive and statistically significant in 2022 and 2023, suggesting that more mixed-use station areas were increasingly associated with recovery in the later period. Distance to center (D-CBD) is mostly insignificant, except for a negative and significant coefficient in 2023. Betweenness centrality (BE) remains positive throughout the period, but shows only limited statistical significance, becoming significant only in 2022. Overall, the VIF values remain below conventional concern thresholds, suggesting no serious multicollinearity among the explanatory variables.

Despite the overall explanatory power of the global OLS models, residual diagnostics reveal significant spatial dependence. Global Moran's I statistics for OLS residuals are positive in all four years (0.048, 0.114, 0.189, and 0.183), with corresponding p-values below conventional significance levels (0.001, 0.002, 0.002 and 0.002). This indicates non-random spatial clustering in the residuals and motivates the use of GWR in the next section to account for spatial heterogeneity.

5.4. GWR results

5.4.1. Model comparison

Table 6 compares the goodness-of-fit of the selected global OLS model and the corresponding GWR model for each year. Overall, GWR consistently outperforms OLS across 2020–2023. In all years, GWR yields lower AICc values and higher adjusted R^2 and R^2 than OLS, indicating improved explanatory power after allowing coefficients to vary spatially. These results suggest that the relationships between ridership change and station attributes are spatially heterogeneous, and that a single global specification is insufficient to capture the observed spatial variation in pandemic-era ridership dynamics.

5.4.2. Summary and maps of GWR local coefficients

Table 7 summarizes the local coefficient estimates from the GWR model by reporting their mean and standard deviation across stations for each year. The results indicate substantial spatial heterogeneity in the estimated relationships, as reflected by non-negligible dispersion in local coefficients for all variables. The maximum local condition numbers for 2020–2023 are 5.938, 5.482, 6.594, and 8.967, respectively, all well below the commonly used threshold of 30. This suggests that local multicollinearity is not a serious concern in the GWR estimations, and the spatial variation in the coefficients is unlikely to be driven by local instability caused by collinearity.

In the following, we map the station-level GWR local coefficients for pre-pandemic ridership (PV), Production and Service (PS), road density (RD), land use mix (LUM), distance to center (D-CBD), and betweenness centrality (BE) for 2020–2023, highlighting spatial variation in both the magnitude and sign of effects across the metro system. We also report the statistical distributions of local coefficients and summarize the shares of positive versus negative coefficients, as well as the proportions that are significantly positive or significantly negative.

Fig. 8 presents the station-level local coefficients for pre-pandemic demand (PV) from 2020 to 2023. The PV coefficients are negative across all stations in every year, indicating that stations with higher pre-pandemic ridership generally experienced larger proportional declines relative to 2019. This negative association is particularly robust in 2020 and 2021, when 100% of stations show statistically significant negative coefficients. In 2022, the relationship remains highly consistent, with 96.6% of stations showing significant negative effects. By 2023, the negative association persists for all stations, but the share of statistically significant negative coefficients decreases to 71.5%, suggesting some weakening or spatial differentiation of the PV effect during the recovery phase.

The maps reveal clear spatial heterogeneity in the magnitude of the PV effect. In 2020 and 2021, stronger negative coefficients are concentrated mainly in and around the central area, with additional pronounced effects extending toward the eastern and southeastern

Table 5
OLS results.

Y (year vs 2019)	PV	PS	LUM	D-CBD	RD	BE
2020	**−0.0142*****	**−0.0409*****	−0.0053	0.0107	**0.0222*****	0.0058
2021	**−0.0182*****	**−0.0395*****	0.0090	0.0011	**0.0199*****	0.0068
2022	**−0.0170*****	**−0.0321*****	**0.0166****	−0.0102	**0.0178*****	**0.0075***
2023	**−0.0199*****	**−0.0270****	**0.0152***	**−0.0166****	**0.0158*****	0.0048
Max VIF	1.3410	4.8707	2.5530	2.6983	1.1636	1.2275

Notes. *, **, *** indicate $p < 0.05$, $p < 0.01$, and $p < 0.001$, respectively. Max VIF reports the maximum VIF for each variable across the four yearly OLS models.

Table 6
GWR vs. OLS.

Model	AICc	Adj. R^2	R^2
OLS			
2020	−628.190410	0.479580	0.494738
2021	−632.983868	0.515968	0.530066
2022	−652.840242	0.462809	0.478455
2023	−622.158715	0.370652	0.388982
GWR			
2020	−635.439529	0.555803	0.621042
2021	−642.250725	0.585236	0.629436
2022	−670.944031	0.594610	0.659567
2023	−638.643963	0.579053	0.674722

Table 7
GWR results.

Year vs 2019	Variable group	4D	Variable	Mean	SD
2020	Pre-pandemic demand		PV	−0.0166	0.0065
	Built environment	Density/Intensity	PS	−0.0402	0.0224
		Diversity	LUM	−0.0038	0.0135
		Destination accessibility	D-CBD	0.0000	0.0273
		Design	RD	0.0238	0.0074
	Centrality		BE	0.0066	0.0064
2021	Pre-pandemic demand		PV	−0.0191	0.0033
	Built environment	Density/Intensity	PS	−0.0373	0.0145
		Diversity	LUM	0.0140	0.0091
		Destination accessibility	D-CBD	−0.0134	0.0261
		Design	RD	0.0199	0.0044
	Centrality		BE	0.0063	0.0036
2022	Pre-pandemic demand		PV	−0.0190	0.0050
	Built environment	Density/Intensity	PS	−0.0270	0.0170
		Diversity	LUM	0.0217	0.0100
		Destination accessibility	D-CBD	−0.0248	0.0317
		Design	RD	0.0157	0.0077
	Centrality		BE	0.0074	0.0044
2023	Pre-pandemic demand		PV	−0.0229	0.0104
	Built environment	Density/Intensity	PS	−0.0222	0.0297
		Diversity	LUM	0.0158	0.0168
		Destination accessibility	D-CBD	−0.0268	0.0333
		Design	RD	0.0148	0.0132
	Centrality		BE	0.0045	0.0086

Notes. Maximum local condition number for years (2020–2023): 5.938, 5.482, 6.594, 8.967

parts of the network. In 2022, the strongest negative effects become more spatially concentrated around the western side of the central city and adjacent inner-urban areas. In 2023, although the western central area remains prominent, strong negative effects also appear in parts of the northern and northwestern network, while several stations in the eastern and southeastern portions become statistically insignificant. Overall, Fig. 8 suggests that pre-pandemic demand remained a consistently negative predictor of ridership recovery, but its spatial influence became less uniformly significant by 2023.

As shown in Fig. 9, the local coefficients for Production and Service (PS) are predominantly negative across the study period, indicating that stations surrounded by higher concentrations of production- and service-oriented activities generally experienced larger proportional ridership declines relative to 2019. This negative relationship is strongest and most spatially consistent in the early pandemic years. In 2020, 95.7% of stations show negative and statistically significant coefficients, while only 4.3% have positive coefficients and none of them are significant. In 2021, the pattern becomes even more uniform, with all stations exhibiting statistically significant negative coefficients. Spatially, the strongest negative PS effects in 2020 and 2021 are concentrated mainly in the southwestern part of the central area, extending along corridors toward the inner-suburban network.

In 2022, the negative association remains present at all stations, but its statistical significance weakens substantially: only 36.2% of stations show significant negative coefficients. The map indicates that significant negative effects become more localized. By 2023, the PS effect becomes more spatially differentiated. Although 71.0% of stations still have negative coefficients, only 34.8% are significantly negative, and 29.0% of stations show positive but non-significant coefficients. Significant negative effects are concentrated in limited clusters. Overall, Fig. 9 suggests that PS intensity was strongly associated with ridership decline during the acute pandemic period, but this relationship weakened and became more localized during the recovery phase.

As shown in Fig. 10, the local coefficients for land use mix (LUM) show a clear transition from a mixed and spatially uneven effect in 2020 to a predominantly positive association during recovery years. In 2020, the LUM effect is divided in sign: 38.2% of stations have positive coefficients, while 61.8% have negative coefficients. However, only a limited share of stations is statistically significant.

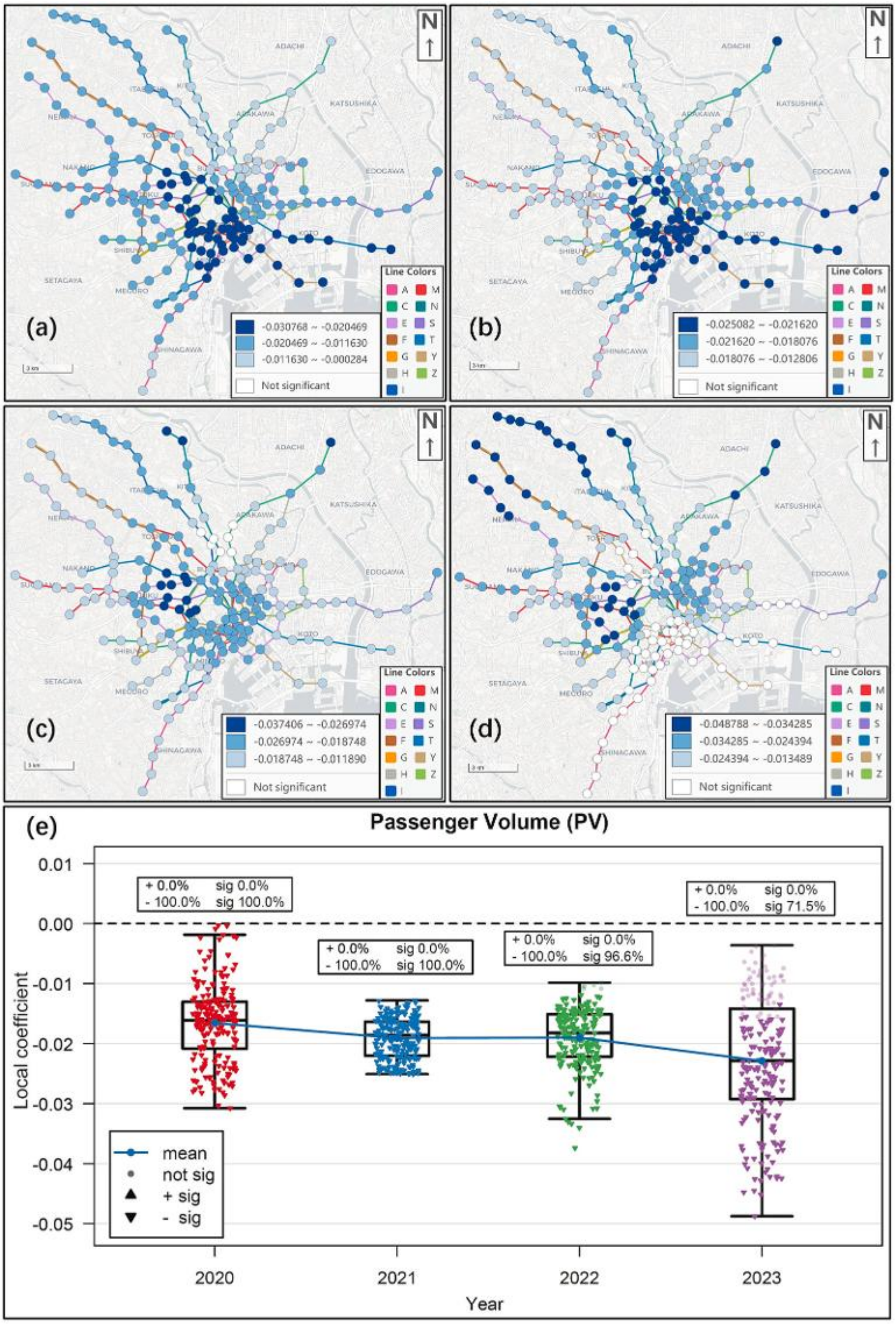

Fig. 8. Spatial distribution of GWR local coefficients for PV in (a) 2020, (b) 2021, (c) 2022, (d) 2023, and (e) yearly distribution of PV local coefficients. In (a)-(d), positive coefficients are shown in red and negative coefficients in blue. (For interpretation of the references to colour in this figure legend, the reader is referred to the web version of this article.)

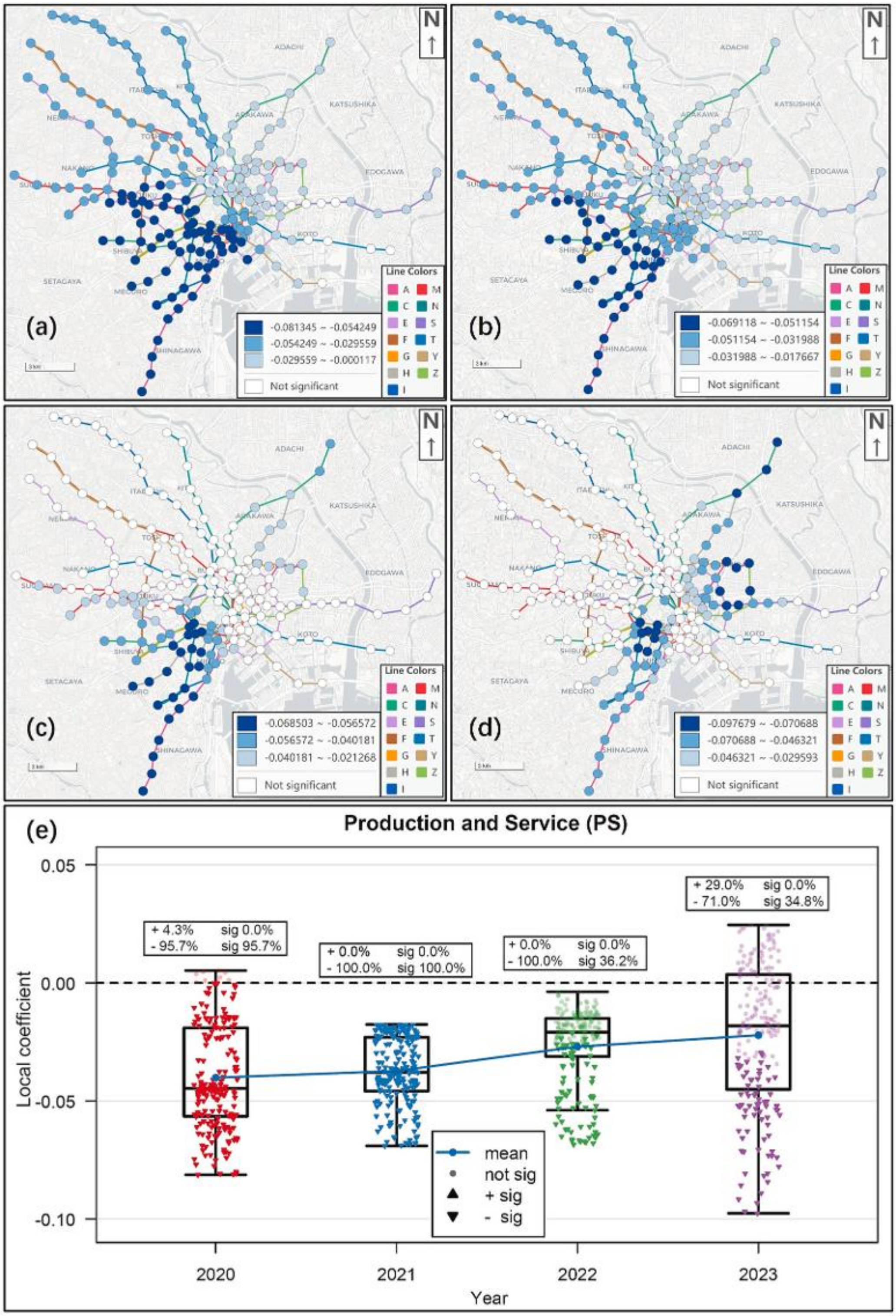

Fig. 9. Spatial distribution of GWR local coefficients for PS in (a) 2020, (b) 2021, (c) 2022, (d) 2023, and (e) yearly distribution of PS local coefficients. In (a)-(d), positive coefficients are shown in red and negative coefficients in blue. (For interpretation of the references to colour in this figure legend, the reader is referred to the web version of this article.)

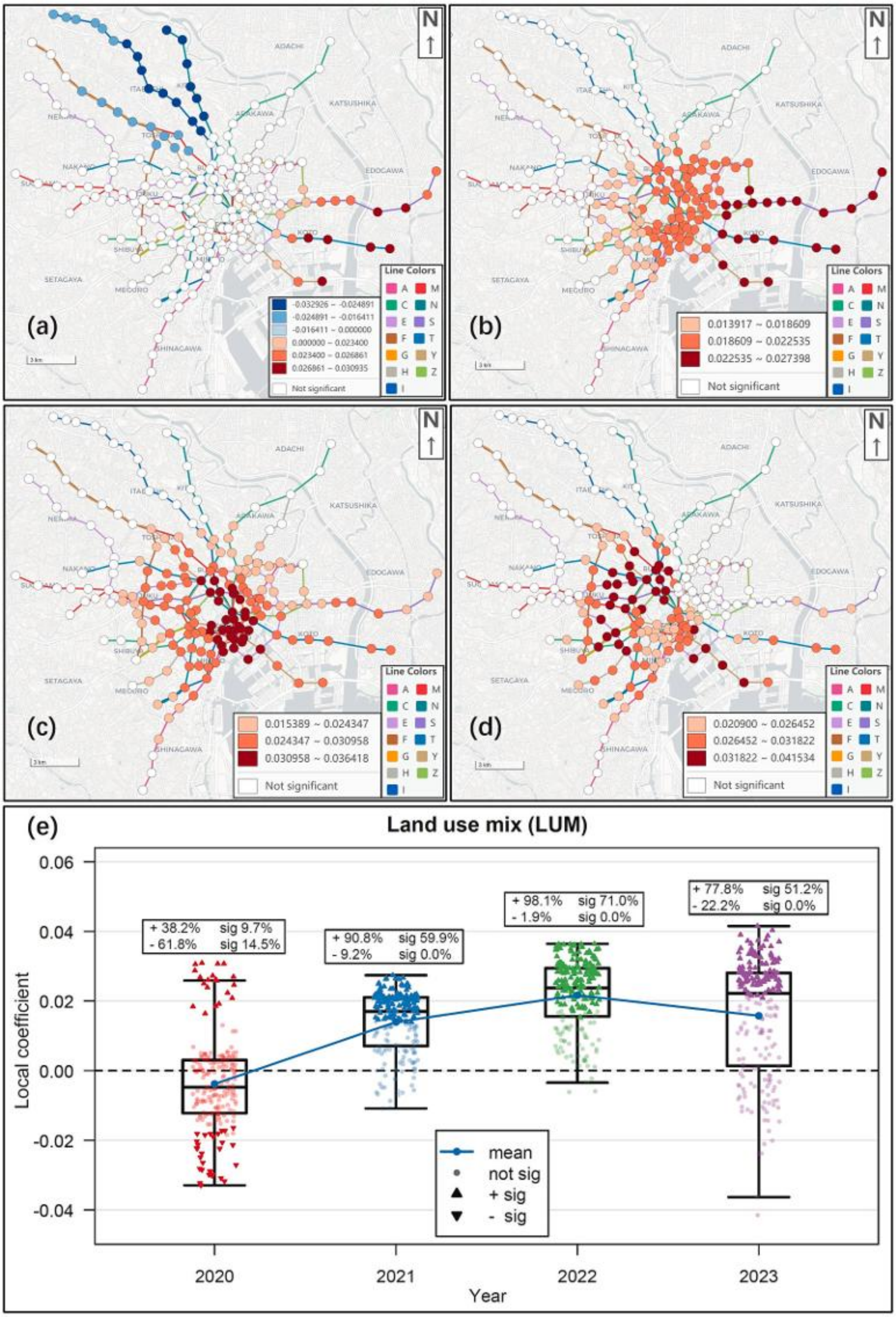

Fig. 10. Spatial distribution of GWR local coefficients for LUM in (a) 2020, (b) 2021, (c) 2022, (d) 2023, and (e) yearly distribution of LUM local coefficients. In (a)-(d), positive coefficients are shown in red and negative coefficients in blue. (For interpretation of the references to colour in this figure legend, the reader is referred to the web version of this article.)

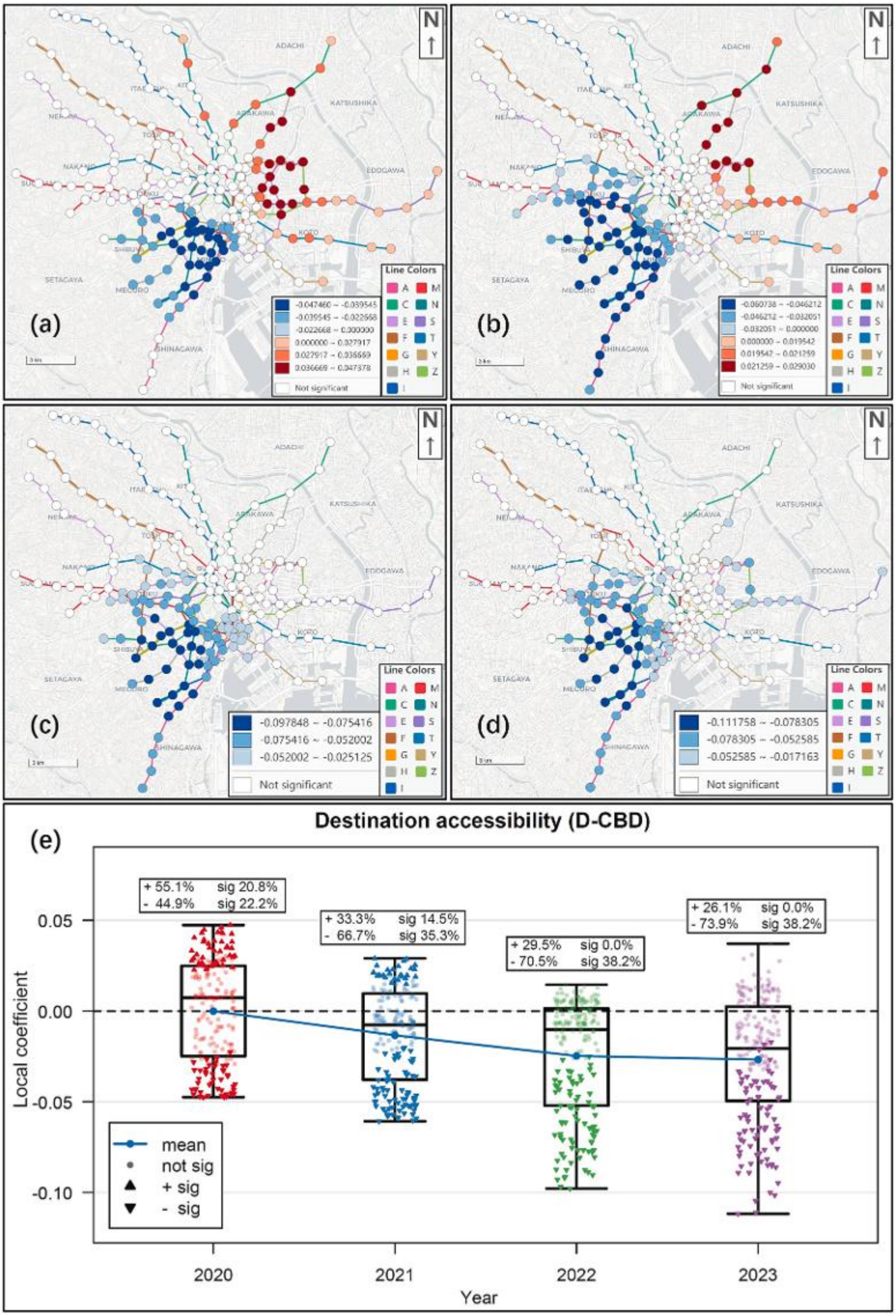

Fig. 11. Spatial distribution of GWR local coefficients for D-CBD in (a) 2020, (b) 2021, (c) 2022, (d) 2023, and (e) yearly distribution of D-CBD local coefficients. In (a)-(d), positive coefficients are shown in red and negative coefficients in blue. (For interpretation of the references to colour in this figure legend, the reader is referred to the web version of this article.)

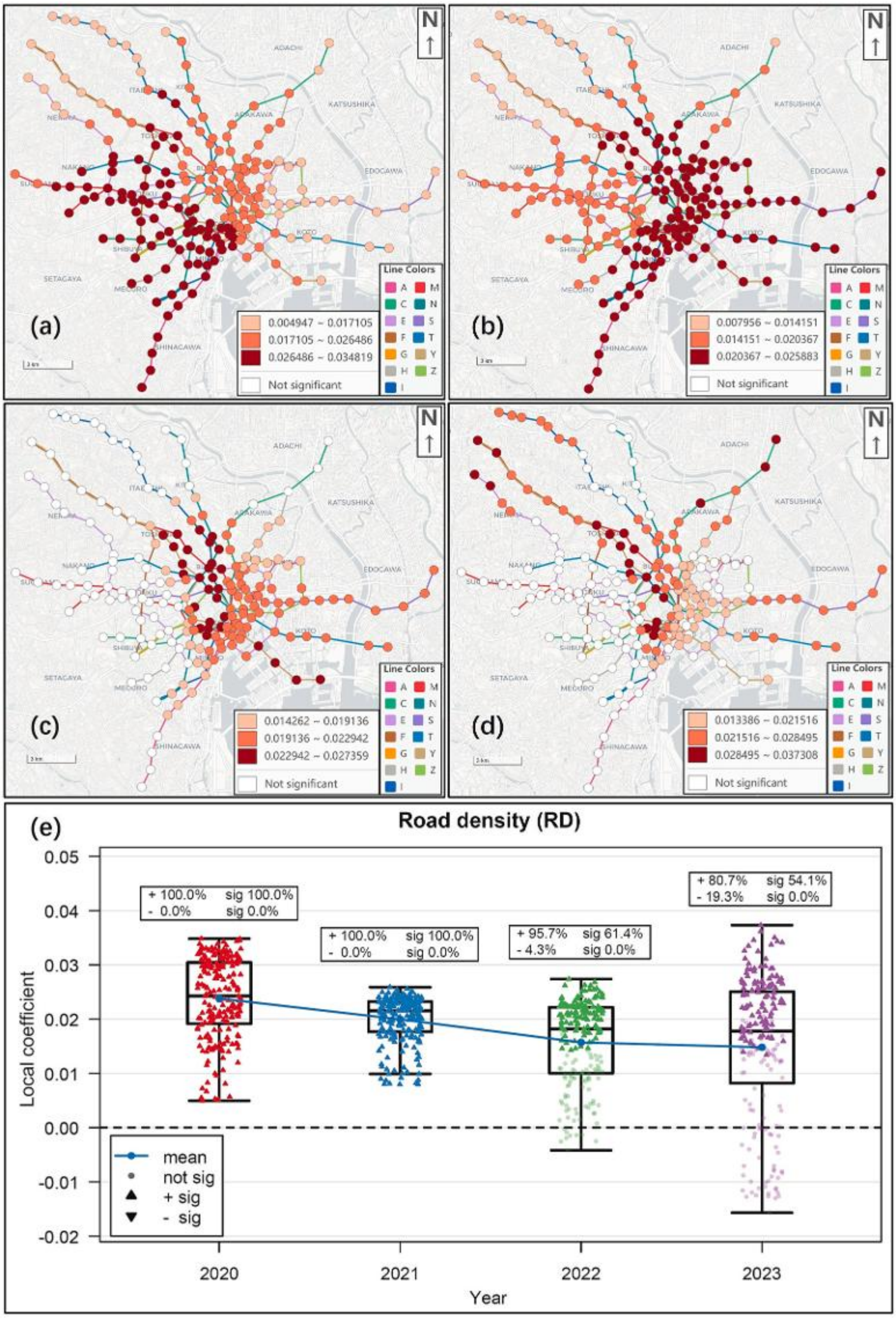

Fig. 12. Spatial distribution of GWR local coefficients for RD in (a) 2020, (b) 2021, (c) 2022, (d) 2023, and (e) yearly distribution of RD local coefficients. In (a)-(d), positive coefficients are shown in red and negative coefficients in blue. (For interpretation of the references to colour in this figure legend, the reader is referred to the web version of this article.)

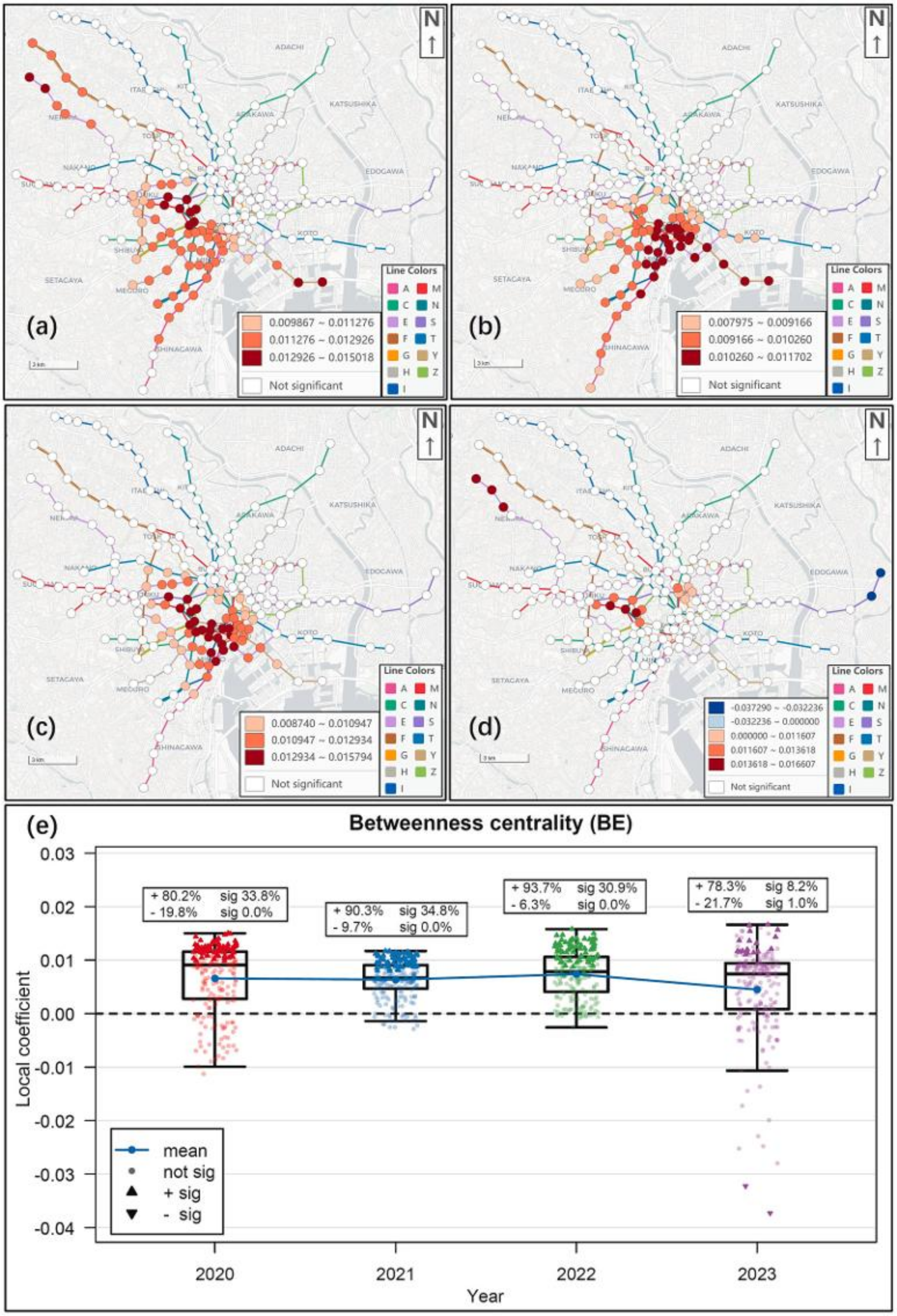

Fig. 13. Spatial distribution of GWR local coefficients for BE in (a) 2020, (b) 2021, (c) 2022, (d) 2023, and (e) yearly distribution of BE local coefficients. In (a)-(d), positive coefficients are shown in red and negative coefficients in blue.

Spatially, significant negative coefficients are mainly observed in part of the northwestern network, whereas positive coefficients appear more clearly toward the eastern side of the network. This suggests that, during the acute pandemic shock, the role of land use mix was highly localized and did not follow a uniform citywide pattern.

From 2021 onward, the LUM effect becomes predominantly positive. In 2021, 90.8% of stations show positive coefficients, and 59.9% are significantly positive. Positive effects are concentrated mainly around the central and eastern parts of the network. In 2022, the positive association becomes even more widespread and robust: 98.1% of stations have positive coefficients, and 71.0% are significantly positive. The strongest positive effects are concentrated in and around the central area. By 2023, LUM remains mostly positive, with 77.8% of stations showing positive coefficients and 51.2% significantly positive, although the spatial pattern becomes more heterogeneous. Overall, Fig. 10 suggests that land use diversity became an increasingly positive factor associated with ridership recovery after 2020, although its influence became spatially differentiated again by 2023.

As shown in Fig. 11, the local coefficients for destination accessibility (D-CBD) exhibit strong spatial heterogeneity and a clear temporal shift in sign. In 2020, the relationship is mixed: 55.1% of stations show positive coefficients and 44.9% show negative coefficients, respectively. Spatially, positive coefficients are mainly concentrated in the eastern and northeastern parts of the network, while negative coefficients are more evident around the southwestern part of the city. The pattern in 2021 is broadly similar to that in 2020, although the negative coefficients become more widespread.

From 2022 onward, the D-CBD effect becomes predominantly negative. In 2022 and 2023, the negative association becomes more pronounced and spatially persistent: 70.5% and 73.9% of stations, respectively, have negative coefficients, and 38.2% of stations in both years show significant negative effects. By contrast, positive coefficients remain present for some stations but are no longer statistically significant in either year. Overall, Fig. 11 suggests that after the initial disruption, stations farther from the central stations tended to experience relatively larger ridership declines, particularly in the southwestern and southern parts of the network.

As shown in Fig. 12, the local coefficients for road density (RD) are predominantly positive throughout the study period, indicating that stations located in denser street networks generally experienced smaller proportional ridership declines and/or stronger recovery. In the early pandemic stage, this positive association is especially strong and spatially pervasive. In 2020, stronger positive effects are concentrated mainly in the western and southwestern parts of the network. The pattern in 2021 remains universally positive and significant, but the strongest coefficients shift somewhat toward the southern and eastern parts of the network, suggesting a broader consolidation of the beneficial role of dense street connectivity.

From 2022 onward, the RD effect remains largely positive but becomes more spatially differentiated. In 2022, 95.7% of stations still show positive coefficients, but only 61.4% are significantly positive. Significant positive effects are concentrated mainly in and around the central area. By 2023, the positive association weakens further in spatial coverage: 80.7% of stations have positive coefficients and 54.1% are significantly positive. The significant positive effects are increasingly concentrated in a more limited set of stations. Overall, Fig. 12 suggests that road density remained a consistently beneficial factor for ridership resilience, but its influence became less uniformly significant and more spatially localized as post-pandemic recovery progressed.

As shown in Fig. 13, the local coefficients for betweenness centrality (BE) are predominantly positive throughout the study period, suggesting that stations occupying more important intermediary positions in the metro network generally tended to experience smaller proportional ridership declines and/or stronger recovery relative to 2019. However, the strength and significance of this relationship vary substantially across space and over time.

In 2020 and 2021, the BE effect is already mainly positive but remains spatially selective. Positive coefficients account for 80.2% of stations in 2020 and 90.3% in 2021, while significantly positive coefficients are observed for 33.8% and 34.8% of stations, respectively. Spatially, significant positive effects are concentrated mainly in the southern part of the central area and nearby corridors, indicating that the resilience advantage associated with network-bridging positions was localized during the early pandemic period. In 2022, the positive association becomes more spatially widespread, with 93.7% of stations showing positive coefficients and 30.9% showing significantly positive effects. These significant positive coefficients remain concentrated mainly around the southern portion of the urban core. By 2023, however, the BE effect weakens markedly. The map shows that significant effects in 2023 are limited to a small cluster of stations, with most stations becoming statistically insignificant. Overall, Fig. 13 suggests that betweenness centrality played a positive but spatially selective role in ridership resilience.

6. Conclusion

6.1. Findings and conclusions

This study examined station-level metro ridership changes in Tokyo during COVID-19, revealing a sharp system-wide demand collapse in 2020 followed by a gradual but incomplete recovery by 2023, alongside substantial station-level heterogeneity in the pace and magnitude of rebound.

Using the proposed modeling framework, the best-performing global specification across years incorporates pre-pandemic ridership (PV), built-environment indicators aligned with the 4D framework (PS, LUM, D-CBD, RD), and network structure (BE). Global OLS estimates indicate that road density (RD) is consistently positive and significant, suggesting that stations embedded in denser street networks tend to experience smaller proportional losses and faster recovery. Pre-pandemic demand (PV) is consistently negative and highly significant, indicating larger proportional declines at high-demand stations. Production and Service (PS) is also negative and significant in every year, although its magnitude weakens over time. Land use mix (LUM) becomes positive and significant only in 2022–2023, while D-CBD is significant only in 2023 and BE only in 2022.

Residual diagnostics further suggest that a single global relationship is insufficient: OLS residuals exhibit significant positive spatial dependence in each year, motivating spatially varying estimation. Consistently, GWR improves model fit in all years, confirming pronounced spatial heterogeneity in how station attributes relate to ridership change. Mapping local GWR coefficients provides a finer-grained interpretation of this heterogeneity. PV local effects are negative for all stations throughout the period, although their significance becomes less uniform by 2023. PS is strongly negative and significant in 2020–2021, but weakens and becomes more localized in 2022–2023. LUM shifts from mixed effects in 2020 to a predominantly positive association from 2021 onward. D-CBD is spatially mixed in 2020–2021 and becomes more predominantly negative from 2022 onward. RD remains largely positive, with significance becoming more localized after 2021. BE is generally positive but spatially selective, with its influence weakening substantially by 2023.

The increasingly positive role of LUM during 2021–2022 can be interpreted as a result of the spatial reorganization of daily activities during the pandemic recovery. In Tokyo, the normalization of telework and hybrid work reduced routine commuting to central employment districts and increased the importance of home-based activity spaces. As residents spent more time near home, daily consumption, services, dining, leisure, and other discretionary activities were more likely to occur around nearby mixed-use station areas rather than CBD-oriented workplace destinations. This behavioral shift helps explain why the LUM effect was spatially mixed in 2020, when mobility was broadly suppressed, but became predominantly positive in 2021 and especially 2022 as urban activity resumed under more localized and flexible mobility patterns.

These findings can also be interpreted through the lens of transit and social resilience. From a transit-resilience perspective, the pandemic represented an external shock that tested the ability of metro stations to absorb disruption, adapt to changing activity patterns, and support gradual recovery. The consistently negative effects of PV and PS suggest that stations strongly dependent on high-volume commuting and production/service-oriented activities were less able to absorb the initial demand shock, because their ridership base was closely tied to centralized employment and routine work trips that were disproportionately reduced during the pandemic. In contrast, the positive and persistent role of RD indicates that stations with denser local street networks had stronger access redundancy and better first-/last-mile connectivity, which may have helped maintain station usability even when overall demand was suppressed.

From a social-resilience perspective, metro recovery is not only a transport performance issue but also reflects the ability of urban neighborhoods to maintain access to daily activities, services, and opportunities during and after disruption. The increasing positive role of LUM after 2020 suggests that mixed-use station areas provided more locally available destinations and supported the reorganization of daily life under telework, hybrid work, and reduced long-distance commuting. In this sense, functional diversity around stations may have helped sustain everyday mobility and neighborhood-level activity recovery. However, because this study does not directly include household-level socio-economic or demographic indicators, the social-resilience interpretation should be understood as an access- and activity-based interpretation rather than direct evidence of social equity outcomes. Future work could further connect station-level ridership resilience with social vulnerability indicators to examine whether resilient station areas also support more equitable access during large-scale disruptions.

More broadly, these results help refine early post-pandemic debates that tended to treat compact urban form and mixed land use primarily as potential sources of infection risk. The findings indicate that different forms of urban concentration had different resilience implications. High pre-pandemic demand and Production and Service intensity remained associated with deeper proportional ridership losses, reflecting the vulnerability of station areas dependent on centralized employment and routine commuting. By contrast, road density was consistently associated with smaller losses, while land-use mix became increasingly positive during the recovery period. This contrast suggests that permeable local access networks and functionally diverse station areas provided the physical conditions through which residents could reorganize daily routines around nearby activities when centralized commuting was disrupted. Such neighborhood-scale adaptive capacity is consistent with the principles of TOD and the 15-Minute City, in which walkable access and a diversity of nearby functions support locally generated mobility and help sustain a baseline level of transit use. The contribution of this study extends beyond explaining the initial ridership shock. It also identifies built-environment conditions associated with later, locally driven recovery. Because these relationships are observational, such station-area characteristics should be understood as complementing rather than replacing top-down operational and financial support.

6.2. Planning and policy implications

The findings provide several implications for strengthening metro resilience and station-area planning under future large-scale disruptions. First, resilience planning should not assume that ridership loss occurs uniformly across the network. Stations with high pre-pandemic demand and high Production and Service intensity experienced larger proportional declines, especially during the early pandemic period. These stations are often major commuting destinations, transfer points, or work/service-oriented activity centers, and their demand is more sensitive to telework, activity restrictions, and changes in centralized employment patterns. For such stations, transit agencies should prepare adaptive operational strategies, including flexible service scheduling, real-time demand monitoring, crowding management, and contingency plans for rapid service adjustment. Rather than applying uniform service reductions, operators should identify stations where demand collapse is likely to be sharp but where a baseline level of service remains socially necessary for essential workers and unavoidable trips.

Second, the consistently positive effect of road density suggests that local access conditions are a key component of station-level transit resilience. Dense and permeable street networks can improve walking access, provide multiple approach routes, and support flexible first-/last-mile connections. Therefore, station-area resilience should be strengthened through improvements to pedestrian environments, intersection safety, bicycle access, bus feeder connections, wayfinding, and barrier-free access. These measures are particularly important for stations where road density or local network permeability is relatively low, because limited access redundancy may make station use more vulnerable when travel behavior changes abruptly. In this sense, transport resilience should be addressed not only within the rail network itself, but also through the surrounding street and access network.

Third, the positive role of land-use mix during the recovery period suggests that mixed-use station areas can support more robust post-disruption recovery. During the pandemic recovery, daily activities became more localized as telework and hybrid work reduced routine commuting to central employment districts. Stations surrounded by diverse functions, such as services, retail, health, community facilities, dining, and leisure opportunities, were better positioned to support neighborhood-based activity recovery. Planning policies should therefore promote functionally mixed station areas rather than highly single-purpose station environments. For employment-dominated or service-intensive station areas that showed stronger ridership losses, planners could encourage a more balanced mix of residential, daily-service, and community-supporting functions to reduce dependence on a single type of trip demand.

Fourth, the spatially uneven effects of D-CBD and BE indicate that proximity to major centers and network-bridging roles alone do not guarantee resilient recovery. Although centrality and accessibility remain important for normal ridership, their effects during disruption are conditional on local urban context and the type of activities surrounding each station. This finding implies that resilience policies should move beyond a simple hierarchy of central versus peripheral stations or hub versus non-hub stations. Instead, the GWR results can be used to identify spatially specific station types, such as high-demand vulnerable stations, work/service-oriented stations with slow recovery, mixed-use stations with stronger recovery potential, and locally accessible stations with robust access networks. Such a classification would allow agencies and planners to prioritize interventions according to each station's local vulnerability and recovery mechanism.

Finally, the results highlight the need to integrate transit resilience with broader social resilience planning. Metro systems support not only commuting efficiency but also access to essential services, local opportunities, and everyday social participation. Maintaining reliable access around stations with socially necessary functions, improving local access networks, and supporting mixed-use neighborhood activity centers can help cities better absorb future shocks, whether caused by pandemics, natural hazards, or other disruptions. In dense transit-oriented cities such as Tokyo, resilience-oriented station-area planning should therefore combine operational preparedness, local access improvement, and land-use diversification. This geographically targeted approach is more appropriate than one-size-fits-all policies because the determinants of ridership loss and recovery vary substantially across space.

6.3. Limitations and future research

This study has several limitations that suggest directions for future work. First, ridership is measured annually at the station level, which is well suited to characterizing medium-term recovery but cannot capture within-year or peak-period dynamics that may be crucial for understanding behavioral mechanisms behind shock and rebound. Future studies could extend the framework using higher-frequency smart-card or mobile-sensing data to distinguish commuting, discretionary travel, and temporal substitution effects more explicitly.

Second, built-environment indicators are constructed using POIs from Foursquare OS Places and a classification procedure to handle missing categories. While POIs offer granular functional information, they may contain classification noise or representation biases, and their temporal attributes may not fully reflect short-term business closures and reopenings during the pandemic. Future research could validate POI-derived measures using complementary land-use datasets, economic activity indicators, or local business registry data.

Third, the recovery metric is an observable outcome that is plausibly influenced by time-varying pandemic context, such as infection waves, vaccination progress, telework adoption, and changes in public-health restrictions. Future work could incorporate epidemiological and policy indicators (e.g., local case/hospitalization measures, mobility restrictions, workplace attendance proxies, or policy stringency indices) and examine whether their effects interact with station-area attributes and network position.

Fourth, although GWR improves fit and reveals rich spatial heterogeneity, the estimated associations should be interpreted as correlational, and unobserved factors (e.g., localized COVID-19 responses, employment composition, modal substitution, and neighborhood socio-demographics) may still contribute to spatially clustered residual structures. Future work could strengthen causal interpretation using quasi-experimental designs, panel approaches with richer controls, or multi-level frameworks that jointly model network structure, built environment, and socio-demographic context. These context-specific conditions also limit direct transferability. Tokyo's dense, polycentric, rail-oriented structure and Japan-specific pandemic responses mean that the findings are most applicable to large, transit-dependent metropolitan areas, while effects may differ in lower-density, more car-dependent, or differently governed cities.

Overall, by integrating pre-pandemic demand, station-area built environment, and network centrality within a spatially explicit modeling framework, this study demonstrates that Tokyo's metro ridership recovery is shaped by both time-varying determinants and persistent spatial heterogeneity, underscoring the need for geographically targeted, context-sensitive interventions to enhance transit resilience under future disruptions.

CRediT authorship contribution statement

Xi Lin: Writing – review & editing, Writing – original draft, Software, Methodology, Data curation, Conceptualization. **Giuseppe Vizzari:** Writing – review & editing, Writing – original draft, Data curation. **Claudio Feliciani:** Writing – review & editing, Conceptualization. **Daichi Yanagisawa:** Writing – review & editing, Supervision, Resources, Conceptualization. **Katsuhiro Nishinari:** Supervision, Resources.

Declaration of generative AI and AI-assisted technologies in the writing process

During the preparation of this work, the authors used GPT-4o at the initial drafting stage and ChatGPT-5.4 during the revision stage to assist with language polishing. After using these tools, the authors reviewed and edited the content as needed and take full responsibility for the content of the publication.

Acknowledgments

Xi Lin was supported by JST SPRING, Grant Number JPMJSP2108.

Claudio Feliciani was supported by JSPS KAKENHI Grant Number JP26K07940.

Daichi Yanagisawa was supported by JSPS KAKENHI Grant Number JP23K21019 and 26H02177.

Giuseppe Vizzari was supported by the Spoke 8 — “Mobility-as-a-Service (MaaS) and Innovative Services,” of the National Center for Sustainable Mobility (MOST), established under the Piano Nazionale di Ripresa e Resilienza (PNRR) — M4C2, Investment 1.4, “Potenziamento strutture di ricerca e creazione di campioni nazionali di R&S su alcune Key Enabling Technologies” funded by the European Union. Project code CN00000023, CUP: D93C22000410001. He was also supported by MUR under the grant “Dipartimenti di Eccellenza 2023–2027” of the Department of Informatics, Systems and Communication of the University of Milano-Bicocca, Italy.

The authors would also like to thank Yuki Oyama for the useful discussion on topics related to this paper.

The authors gratefully acknowledge the three anonymous reviewers for their valuable comments and constructive suggestions, which contributed to improving the clarity and quality of this manuscript.

Data availability

Data will be made available on request.

References

An, D., Tong, X., Liu, K., Chan, E.H.W., 2019. Understanding the impact of built environment on metro ridership using open source in Shanghai. Cities 93, 177–187. https://doi.org/10.1016/j.cities.2019.05.013.

Andersson, D.E., Shyr, O.F., Yang, J., 2021. Neighbourhood effects on station-level transit use: evidence from the Taipei metro. J. Transp. Geogr. 94, 103127. https://doi.org/10.1016/j.jtrangeo.2021.103127.

Balbontin, C., Hensher, D.A., Beck, M.J., Giesen, R., Basnak, P., Vallejo-Borda, J.A., Venter, C., 2021. Impact of COVID-19 on the number of days working from home and commuting travel: a cross-cultural comparison between Australia, South America and South Africa. J. Transp. Geogr. 96, 103188. https://doi.org/10.1016/j.jtrangeo.2021.103188.

Basu, R., Ferreira, J., 2021. Sustainable mobility in auto-dominated Metro Boston: challenges and opportunities post-COVID-19. Transp. Policy 103, 197–210. https://doi.org/10.1016/j.tranpol.2021.01.006.

Chang, H.-H., Lee, B., Yang, F.-A., Liou, Y.-Y., 2021. Does COVID-19 affect metro use in Taipei? J. Transp. Geogr. 91, 102954. https://doi.org/10.1016/j.jtrangeo.2021.102954.

Chava, J., Newman, P., Tiwari, R., 2018. Gentrification of station areas and its impact on transit ridership. Case Studies Transport Policy 6, 1–10. https://doi.org/10.1016/j.cstp.2018.01.007.

Chen, C., Chen, J., Barry, J., 2009. Diurnal pattern of transit ridership: a case study of the New York City subway system. J. Transp. Geogr. 17, 176–186. https://doi.org/10.1016/j.jtrangeo.2008.09.002.

Cui, M., Yu, L., Dai, Z., Wu, Y., Wang, Y., Cao, J., 2025. Metro ridership recoverability and the built environment: Exploring station-level non-linear impacts. Transp. Res. Part D: Transp. Environ. 147, 104852. https://doi.org/10.1016/j.trd.2025.104852.

de Palma, A., Vosough, S., Liao, F., 2022. An overview of effects of COVID-19 on mobility and lifestyle: 18 months since the outbreak. Transp. Res. A Policy Pract. 159, 372–397. https://doi.org/10.1016/j.tra.2022.03.024.

Ding, C., Cao, X., Liu, C., 2019. How does the station-area built environment influence Metrorail ridership? using gradient boosting decision trees to identify non-linear thresholds. J. Transp. Geogr. 77, 70–78. https://doi.org/10.1016/j.jtrangeo.2019.04.011.

Gan, Z., Yang, M., Feng, T., Timmermans, H.J.P., 2020. Examining the relationship between built environment and metro ridership at station-to-station level. Transp. Res. Part D: Transp. Environ. 82, 102332. https://doi.org/10.1016/j.trd.2020.102332.

Gao, F., Yang, L., Han, C., Tang, J., Li, Z., 2022. A network-distance-based geographically weighted regression model to examine spatiotemporal effects of station-level built environments on metro ridership. J. Transp. Geogr. 105, 103472. https://doi.org/10.1016/j.jtrangeo.2022.103472.

Kalkstein, A.J., Kuby, M., Gerrity, D., Clancy, J.J., 2009. An analysis of air mass effects on rail ridership in three US cities. J. Transp. Geogr. 17, 198–207. https://doi.org/10.1016/j.jtrangeo.2008.07.003.

Kamga, C., Eickemeyer, P., 2021. Slowing the spread of COVID-19: Review of “Social distancing” interventions deployed by public transit in the United States and Canada. Transp. Policy 106, 25–36. https://doi.org/10.1016/j.tranpol.2021.03.014.

Karawapong, A., Karoonsoontawong, A., Kanitpong, K., 2025. Exploring the multiscale relationship between the built environment and metro station ridership. Case Studies Transport Policy 20, 101466. https://doi.org/10.1016/j.cstp.2025.101466.

Kashem, S.B., Baker, D.M., González, S.R., Lee, C.A., 2021. Exploring the nexus between social vulnerability, built environment, and the prevalence of COVID-19: a case study of Chicago. Sustain. Cities Soc. 75, 103261. https://doi.org/10.1016/j.scs.2021.103261.

Kim, J., Kwan, M.-P., 2021. The impact of the COVID-19 pandemic on people's mobility: a longitudinal study of the U.S. from March to September of 2020. J. Transp. Geogr. 93, 103039. https://doi.org/10.1016/j.jtrangeo.2021.103039.

Li, J., Pan, H., Liu, W., Chen, Y., 2024a. Exploring the relationship between the determinants and the ridership decrease of urban rail transit station during the COVID-19 pandemic incorporating spatial heterogeneity. J. Rail Transport Plann. Manage. 32, 100482. https://doi.org/10.1016/j.jrtpm.2024.100482.

Li, L., Zhong, L., Ran, B., Du, B., 2024b. Analysis of the relationship between metro ridership and built environment: a machine learning method considering combinational features. Tunn. Undergr. Space Technol. 144, 105564. https://doi.org/10.1016/j.tust.2023.105564.

Li, M., Guo, W., Guo, R., He, B., Li, Z., Li, X., Liu, W., Fan, Y., 2022. Urban network spatial connection and structure in China based on railway passenger flow big data. Land 11, 225. https://doi.org/10.3390/land11020225.

Li, M., Rodriguez, D.A., 2024. Marked crosswalks, station area built environments, and transit ridership: Associations between changes in 877 US TOD stations, 2010–2018. Transp. Res. A Policy Pract. 179, 103926. https://doi.org/10.1016/j.tra.2023.103926.

Li, S., Lyu, D., Liu, X., Tan, Z., Gao, F., Huang, G., Wu, Z., 2020. The varying patterns of rail transit ridership and their relationships with fine-scale built environment factors: big data analytics from Guangzhou. Cities 99, 102580. https://doi.org/10.1016/j.cities.2019.102580.

Li, Z., Tang, J., Ji, Y., Liang, X., Hu, L., Hu, C., 2025. Relationship between the built environment and metro usage patterns: a motif-based perspective. Tunn. Undergr. Space Technol. 159, 106488. https://doi.org/10.1016/j.tust.2025.106488.

Liu, L., Miller, H.J., Scheff, J., 2020. The impacts of COVID-19 pandemic on public transit demand in the United States. PLoS One 15, e0242476. https://doi.org/10.1371/journal.pone.0242476.

Mizutori, M., 2025. The ethos of the Sendia framework must continue to evolve. Int J Disaster Risk Sci 16, 6. https://doi.org/10.1007/s13753-025-00618-5.

Moghimi, B., Kamga, C., Safikhani, A., Mudigonda, S., Vicuna, P., 2023. Non-stationary time series model for station-based subway ridership during COVID-19 pandemic: case study of New York City. Transp. Res. Rec. 2677, 463–477. https://doi.org/10.1177/03611981221084698.

Pang, L., Jiang, Y., Wang, J., Qiu, N., Xu, X., Ren, L., Han, X., 2023. Research of metro stations with varying patterns of ridership and their relationship with built environment, on the example of Tianjin, China. Sustainability 15, 9533. https://doi.org/10.3390/su15129533.

Sabbah, T., Selamat, A., Selamat, M.H., Al-Anzi, F.S., Viedma, E.H., Krejcar, O., Fujita, H., 2017. Modified frequency-based term weighting schemes for text classification. Appl. Soft Comput. 58, 193–206. https://doi.org/10.1016/j.asoc.2017.04.069.

Shao, Q., Zhang, W., Cao, X., Yang, J., Yin, J., 2020. Threshold and moderating effects of land use on metro ridership in Shenzhen: implications for TOD planning. J. Transp. Geogr. 89, 102878. https://doi.org/10.1016/j.jtrangeo.2020.102878.

Shi, Y., Yin, C., Long, Y., Wen, J., Fan, L., 2025. Residential preferences and purpose-specific walking behaviors: Mediation effects of built environments. Transp. Res. Part D: Transp. Environ. 149, 105067. https://doi.org/10.1016/j.trd.2025.105067.

Singhal, A., Kamga, C., Yazici, A., 2014. Impact of weather on urban transit ridership. Transp. Res. A Policy Pract. 69, 379–391. https://doi.org/10.1016/j.tra.2014.09.008.

Su, S., Wang, Z., Li, B., Kang, M., 2022. Deciphering the influence of TOD on metro ridership: an integrated approach of extended node-place model and interpretable machine learning with planning implications. J. Transp. Geogr. 104, 103455. https://doi.org/10.1016/j.jtrangeo.2022.103455.

Thomas, F.M.F., Charlton, S.G., Lewis, I., Nandavar, S., 2021. Commuting before and after COVID-19. Transp. Res. Interdiscip. Perspect. 11, 100423. https://doi.org/10.1016/j.trip.2021.100423.

Tu, W., Cao, R., Yue, Y., Zhou, B., Li, Q., Li, Q., 2018. Spatial variations in urban public ridership derived from GPS trajectories and smart card data. J. Transp. Geogr. 69, 45–57. https://doi.org/10.1016/j.jtrangeo.2018.04.013.

Vickerman, R., 2021. Will Covid-19 put the public back in public transport? A UK perspective. Transp. Policy 103, 95–102. https://doi.org/10.1016/j.tranpol.2021.01.005.

Wilbur, M., Ayman, A., Sivagnanam, A., Ouyang, A., Poon, V., Kabir, R., Vadali, A., Pugliese, P., Freudberg, D., Laszka, A., Dubey, A., 2023. Impact of COVID-19 on Public Transit Accessibility and Ridership. Transp. Res. Rec. 2677, 531–546. https://doi.org/10.1177/03611981231160531.

Xiao, W., Wei, Y.D., Wu, Y., 2022. Neighborhood, built environment and resilience in transportation during the COVID-19 pandemic. Transp. Res. Part D: Transp. Environ. 110, 103428. https://doi.org/10.1016/j.trd.2022.103428.

Yan, J., Wan, Q., Feng, J., Wang, J., Hu, Y., Yan, X., 2023. The non-linear influence of built environment on the school commuting metro ridership: the case in Wuhan. China. ISPRS International Journal of Geo-Information 12, 193. https://doi.org/10.3390/ijgi12050193.

Yang, H., Lu, Y., Wang, J., Zheng, Y., Ruan, Z., Peng, J., 2023a. Understanding post-pandemic metro commuting ridership by considering the built environment: a quasi-natural experiment in Wuhan, China. Sustain. Cities Soc. 96, 104626. https://doi.org/10.1016/j.scs.2023.104626.

Yang, L., Yu, B., Liang, Y., Lu, Y., Li, W., 2023b. Time-varying and non-linear associations between metro ridership and the built environment. Tunn. Undergr. Space Technol. 132, 104931. https://doi.org/10.1016/j.tust.2022.104931.

Zhang, J., Hayashi, Y., Frank, L.D., 2021. COVID-19 and transport: Findings from a world-wide expert survey. Transp. Policy 103, 68–85. https://doi.org/10.1016/j.tranpol.2021.01.011.

Zhao, J., Deng, W., Song, Y., Zhu, Y., 2014. Analysis of Metro ridership at station level and station-to-station level in Nanjing: an approach based on direct demand models. Transportation 41, 133–155. https://doi.org/10.1007/s11116-013-9492-3.

Zhao, J., Deng, W., Song, Y., Zhu, Y., 2013. What influences Metro station ridership in China? Insights from Nanjing. Cities 35, 114–124. https://doi.org/10.1016/j.cities.2013.07.002.

Ziedan, A., Brakewood, C., Watkins, K., 2023. Will transit recover? a retrospective study of nationwide ridership in the United States during the COVID-19 pandemic. J. Public Transp. 25, 100046. https://doi.org/10.1016/j.jpubtr.2023.100046.